Buckling Behavior of Functionally Graded Doubly Curved Spherical and Cylindrical Shells

A Dissertation Submitted
in partial Fulfillment of the Requirements
for the Award of the Degree of

MASTER OF ENGINEERING

in

CAD/CAM Engineering

by

Ritu Raj Rajpoot

801684011

Under Supervision of:

Dr. Neeraj Grover
Assistant Professor
Mechanical Engineering Department

Dr. Kishore Khanna
Assistant Professor
Mechanical Engineering Department

MECHANICAL ENGINEERING DEPARTMENT
THAPAR INSTITUTE OF ENGINEERING AND TECHNOLOGY
(DEEMED TO BE UNIVERSITY), PATIALA-147004, PUNJAB, INDIA
July 2018

Dedicated To

My Parents

Certificate

This is to certify that the work done in this thesis report titled **"Buckling Behavior of Functionally Graded Doubly Curved Spherical and Cylindrical Shells"** submitted in partial fulfillment of requirement for the award of Master of Engineering degree in CAD/CAM Engineering in the Mechanical Engineering Department of Thapar Institute of Engineering and Technology, Patiala, is an authentic record of work carried out by me under the guidance of **Dr. Neeraj Grover** and **Dr. Kishore Khanna**, Mechanical Engineering Department, Thapar Institute of Engineering and Technology, Patiala. The matter embodied in this report has not been submitted in any part or full to any other university or institute for the award of any degree.

Ritu Raj

Ritu Raj Rajpoot

Roll. No. 801684011

This is to certify that above declaration made by the student concerned is correct to the best of my knowledge and belief.

Approved

Dr. Neeraj Grover
Assistant Professor
MED
Dated: Aug 03, 2018

Dr. Kishore Khanna
Assistant Professor
MED
Dated: Aug 03, 2018

Acknowledgement

I would like to extend my sincere and heartfelt gratitude to all those who helped me in completing the thesis report. Firstly, I would like to thank Dr. Neeraj Grover and Dr. Kishore Khanna for their continuous support, time and encouragement throughout the course of this study. I have learned about so many new things from them and look forward to their continuous support in the future as well.

Lastly, I would like to thank my parents, family and friends for their unconditional love and moral support in finalizing this report within the limited time frame.

Ritu Raj

Ritu Raj Rajpoot

ABSTRACT

Functionally Graded Materials (FGM) is an advance material with varying properties across the thickness. The overall properties of the material can be altered according to its different applications. FGM shells and plates are being used in various sectors of engineering, military, medical, construction, chemical industries. Wide use of FGM makes it an area of research for better development of machinery, equipment and many more. For few decades, the researches had done taking different solving methods and deformation theories to get the best results for FGM shells and plates. Buckling response of FGM shells are being discussed and modelled using inverse hyperbolic shear deformation theory. The mentioned theory based upon a shear strain function which satisfies the criteria of continuity and differentiability, also satisfies traction free boundary conditions. The governing equations are solved using principle of virtual work. The solution methodology used is Navier type exact solution. Results are provided for plates, thin and thick shells. Also, finite element method is implemented to analyze the buckling response of the FGM doubly curved spherical and cylindrical shells and the eigenvalue solution method is used to get the non-dimensionality buckling results. Results obtained for closed-form solutions as well as numerical method are validated and compared with each other to examine the accuracy of the generalized code and the comparison of analytical results and additionally done with the existing close-form results.

Keywords: FGM shells, Buckling, Closed-form solutions, Inverse hyperbolic shear deformation theory, FEM

Table of Contents

List of Figures

List of Tables

Nomenclature

x_1,x_2,x_3	Cartesian coordinates
$\bar{u}$, $\bar{v}$, $\bar{w}$	In-plane displacements
u,v,w	Mid-plane displacements
a,b,h	Length, breadth and thickness of shell
R_1,R_2	Radius of curvature
R	Constant
a_1,a_2	Vector tangents
$[\bar{Q}_{ij}]^{(k)}$	Transformed reduced stiffness matrix
E	Elasticity coefficient
G	Rigidity coefficient
N	Poisons ratio
U	Strain energy
V	Work done
N,M,P	In-plane stress, moment and higher order moment resultant
R	Resultant stiffness matrix
F	Force vector
K_G	Global geometric stiffness matrix
G	Geometric stiffness matrix
Q	Transverse load

Greek Symbols

ϕ_1 , ϕ_2	Shear rotations
Θ	Angle of fibre orientation
ε_1 , ε_2	Normal strains
ε_6	In-plane shear strain
ε_4 , ε_5	Transverse shear strains
ξ_1, ξ_2, ξ_3	Surface coordinates
$\varepsilon_L, \varepsilon_{NL}$	Linear strain and non-linear strain
Λ	Buckling load parameter
Σ	Normal stress
Δ	Displacement vector

Acronyms

CLPT	Classical laminate plate theory
FSDT	First order shear deformation theory
HSDT	Higher order shear deformation theory
IHSDT	Inverse hyperbolic shear deformation theory
CFS	Closed form solution
SSSS	Simply supported boundary condition
CCCC	Clamped boundary condition
CLT	Classical plate theory
NDBP	Non-dimensional buckling parameter

CHAPTER 1 INTRODUCTION

For the last few decades, the need for the improvements in the material has increased due to technology advancement. Pure metals had a very limited applications in the various engineering sectors due to the need for the conflicting properties of the material. For example, an application may require a material whose properties consists of ductility as well as hardness, there is no such natural occurring material. So, to solve this kind of problems combinations of materials with one another are used. At first, this type of combinations is used for alloys but the limitation was for alloying there is a limit to which one material can be dissolved into another because of thermodynamic equilibrium limit. Then the composite material is introduced, it shows excellent combinations of materials and the properties of the composites are different from its individual material and also light in weight but under extreme conditions the material fails due to delamination. The advance class of composite material was developed with varying properties across the changing dimension. These materials are called Functionally Graded Material (FGM). The various applications of material in the form of plates and shells can be beneficial for the development.

1.1 Plates and Shells

The plates and shells are the types of structural element used for aerospace, engine, constructions, etc. The plate is a thin and two-dimensional flat structural element with very small thickness compared to other planar dimensions. Shell is used to describe the structural element which possess strength and rigidity because of its thin and curved form. It is also a three dimensional solid with very small thickness as plates but the difference is that the middle surface is formed as a curved surface and can be singly curved or doubly curved. Plates are the special case of shells as when curvature ratio is equals to infinity, the shells tend to behave as the plate. Plates and shells have a wide application in many sectors i.e. building structures, pressure vessels, etc.

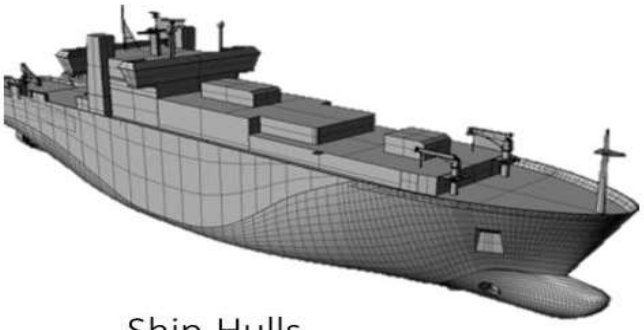

Ship Hulls

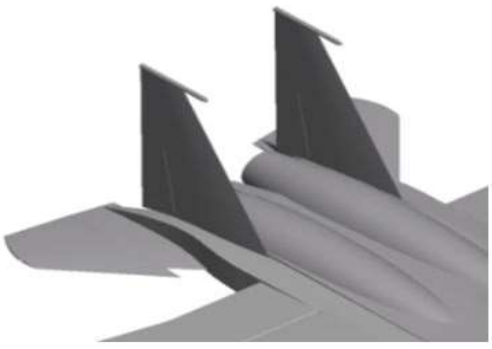

Aircraft Skins

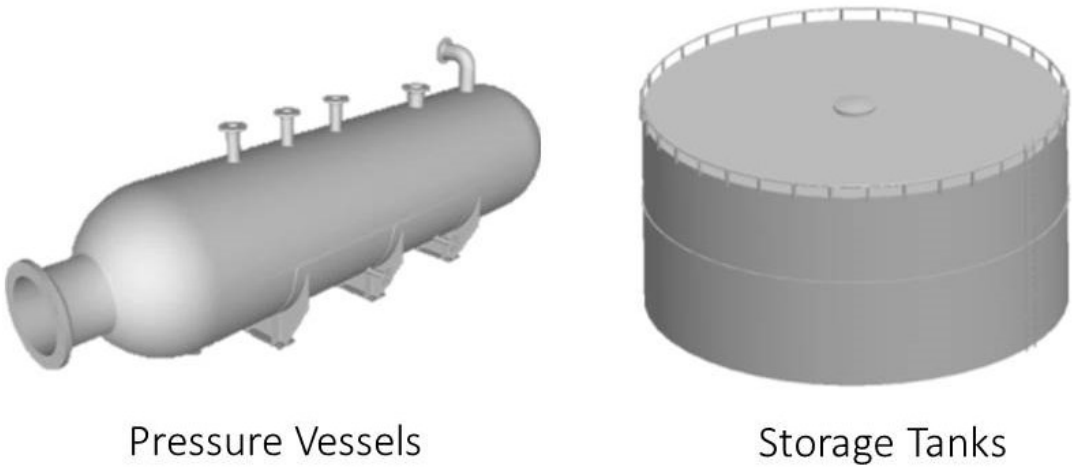

Figure 1.1 Applications of plates and shells in different sectors [1]

1.2 Composite Materials

For the past few decades, material science is rapidly progressing for betterment of the materials and their application in various sectors of engineering. The need to use the properties of different material into one for fulfillment of the desired properties essential for the particular applications has led to the development of alloys and composite materials. Alloys are defined as the material which are made by combining two or more materials into one to give greater strength or resistance to corrosion. But alloys have disadvantages as two similar materials that are similar in nature like metal/metal and non-metal/non-metal. Whereas in composites, the material components used can be different from one another chemically and physically. The composite materials are made by combining two or more constituent materials at macro levels consisting different properties to make a new material whose properties are totally different from the individual materials.

The composites materials are preferred over other materials for various applications because of their superior properties as they are stronger, lighter and less expensive than traditional materials and alloys. They are usually used for buildings, bridges and many engineering structures. Earlier, brick was the first composite material used for building construction which consists mud and straw as a binder. The first artificial composite made in 1907 was Bakelite and commonly used composite is fiberglass for its stiffness, strength and ductile properties. Composite material consists matrix and reinforcement. Matrix acts as binder to support material of the reinforcement used for strengthening the material. To enhance the properties of the matrix, reinforcements with their special mechanical and physical properties is provided to the composite material. Example of matrices are polyester resin, vinyl ester resin, epoxy resin

etc. Examples of reinforcement are fiber, particles and cores. A composite material is classified into three i.e. fibrous, particulate and structural composites.

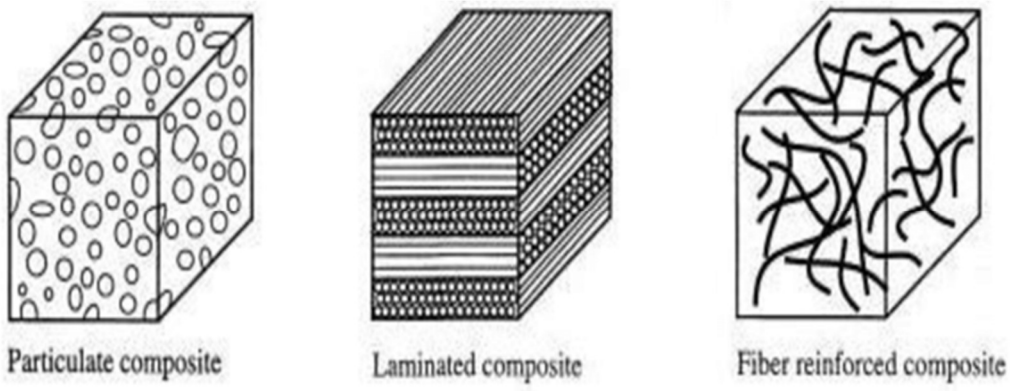

Figure 1.2 Types of composite materials [2]

1.3 Functionally Graded Materials

Functionally Graded Materials (FGMs) are a class of advance materials and are characterized by the variation in the properties over changing dimension according to power law or exponential law. Initially they were developed as a thermal barrier for aerospace structures and fusion reactors. The examples of FGM which occurs in nature are bones, skin, teeth, bamboo, etc. The FGM may be composed of ceramic/metal, ceramic/ceramic, ceramic/glass, ceramic/polymer etc. Aluminum/Alumina, Alumina/Zirconia, Mullite/Alumina, etc. are examples of manufactured FGMs. The material properties can be tailored according to the application and working conditions which makes it preferable for many applications. The gradual change in the microstructure of FGM makes it different from composite materials, which have an irregularity in mechanical properties due to two distinct materials bonded together. Thus, this results in the delamination of composite materials at high thermal loading and cracks will appear at the interface making them vulnerable. In FGMs, these issues are minimized by changing the material properties progressively. It has a graded interface unlike sharp interface present in the composite materials. Further, the main aim of production of FGM is to eliminate the macroscopic boundary of materials in which properties of material changes continuously. It has a characteristic in which the properties can be tailored according to the need of the application. The concept of FGM was developed to remove the sharp interface that exist in the composite material and to replace it with continuous change in the interface.

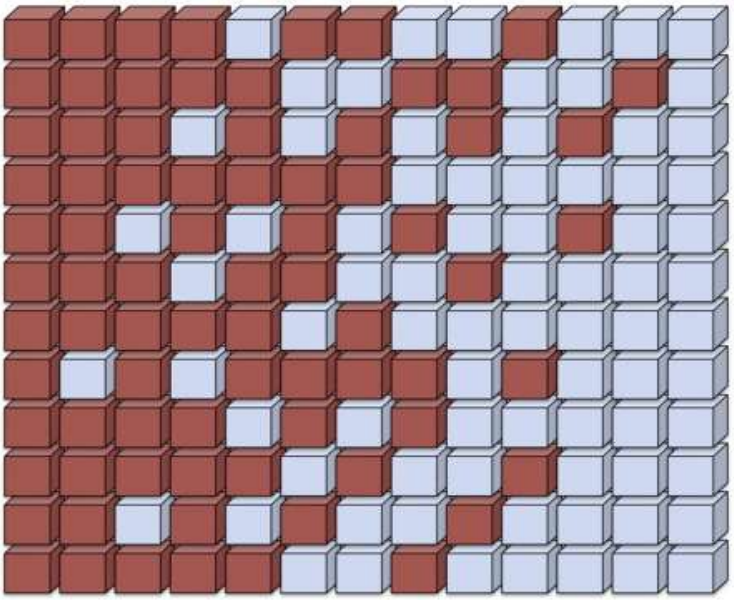

Figure 1.3 Varying material property in FGM [Sola *et al.* (2016)]

1.4 Types of Functionally Graded Materials

Functionally graded material can be designed as continuous-graded structure and some are as step-wise structures according to their application. Thus, they are classified according to their application depending on the properties of the materials as follows:

a) Microstructure Gradient FGM are the materials that are designed so that the different microstructure can be produced to achieve the required material properties which is changing continuously across the dimension.

b) Porosity Gradient FGM are the material in which porosity is made to change with the change in the spatial position in bulk material. According to the application of this type of FGM, the shape and size of the pores are varied. Its wide application is in the biomedical sector for making the body parts for the implantation because of its resemblance to the bone structure.

c) Chemical Composition Gradient FGMs in which composition of the material varies chemically and it can be in the form of single or multiphase. Single phase usually occurs due to sintering whereas multiphase is made to change the properties across the bulk volume of the material.

1.5 Applications

With the increase in the researches in the field of the FGM, its application has been increased over a period of time. As it offers very promising applications even in the harsh operating conditions thus, it's being applied in various industrial sectors. Few of those applications are listed below: -

a. Aerospace Industry: - At initial level of application of FGM, they were developed for space plane bodies because of their better thermal insulation properties. In aerospace FGM materials is used for space shuttles,
b. Automobile Industry: - FGMs are developed very rapidly over few years but still their use in automobile industry is limited due to their high production cost and only used for most important parts.

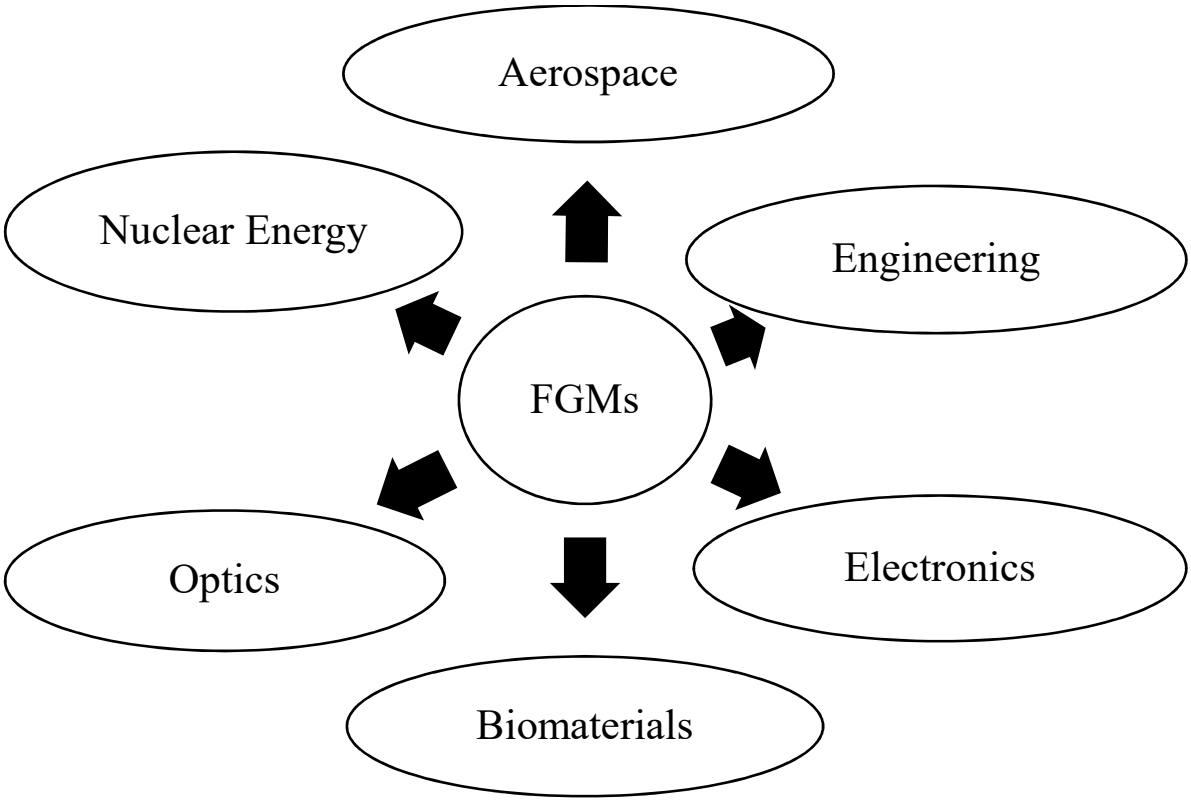

Figure 1.4 Various applications of FGM

c. Biomedical: - As FGMs occurs in human body as well in bone and teeth it's easy to replace them with manufactured FGM when any damage happens or because of natural ageing process.
d. Energy Industry: - To improve the efficiency of some of the equipment in energy industries, FGM are needed.

1.6 Buckling

Buckling is a mode of failure which can be defined as a sudden lateral deflection due to the applied load i.e. axial compressive load large enough to make the structure member unstable. Two techniques are used to predict the buckling load are non-linear buckling analysis and eigenvalue or linear buckling analysis. Non-linear buckling analysis is usually recommended for evaluation or design of actual structures whereas buckling analysis via eigenvalue estimate the buckling strength theoretically for an ideal elastic structure. Both methods show different

results from each other so, it is necessary to know the difference for where to use them. Examples of buckling are compressive members in bridges, overload metal building columns, hull of submarine, pressure vessels, roof trusses, etc.

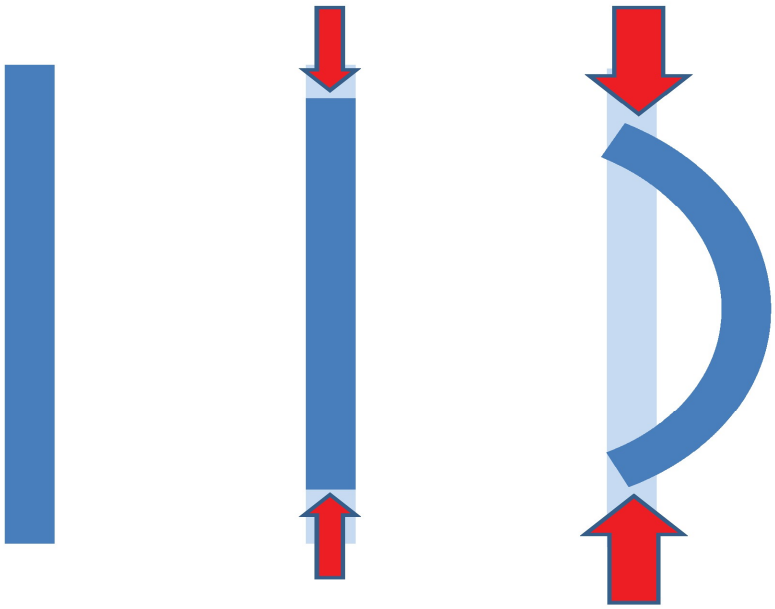

Figure 1.5 Buckling of a column [3]

1.6 Modelling of FGM

Functionally graded materials are studied to evaluate the behavior under different loading and boundary conditions based upon their applications. The material gradation properties various continuously according to two laws i.e. exponential and power. The modeling of FGM shells are done using two approaches. In analytical and finite element method, the shear deformation theory based upon inverse hyperbolic function is used for the mathematical modelling of FG shells and the governing differential equations are acquired by principle of virtual work and Navier type exact solution is used. Finite element method has been developed over the years, it can generate accurate results even for a complex problem by dividing it to small elements.

Summary

The gradual change of the FG material properties makes it more adaptable to the different application in different sectors. In this chapter, the applications and types are being discussed and how FGM are more suitable than composite material and they can be further advanced for the future work.

CHAPTER 2 LITERATURE REVIEW

2.1 Introduction

This section explains discussion of an existing literature on advance material i.e. functionally graded materials. They are increasingly being used in aerospace, automobiles, marine etc. FGMs are advance class of composite materials, whose properties vary gradually across the dimension. With the development in technology, FGMs have become an area of interest by many researchers for development of new theories, methods and approaches for analysis of static, buckling and vibration response. The literature review has been carried out on materials on the basis of the development of the theories during the past and the approaches being used to characterize the response of FG plates and shells.

2.2 Development of Theories

Over the years, many ways for modelling the materials were introduced by the researchers in order to study the complicating effects of the materials. Love (1927) developed the first simple equivalent single layer theory (ESL) known as classical plate theory (CPT) using the Kirchhoff's hypothesis. Classical laminated plate theory (CLPT) was introduced by Reissner and Stavsky (1961) and implemented the classical plate theories on the laminated structures. This theory shows inaccuracy as it ignores the transverse strains but still gives the good results for thin plates.

Displacement field given according to CLPT:

$$\begin{aligned} u(x,y,z) &= u_0(x,y) - z\frac{\partial w_0}{\partial x} \\ v(x,y,z) &= v_0(x,y) - z\frac{\partial w_0}{\partial y} \\ w(x,y,z) &= w_0(x,y) \end{aligned} \tag{2.1}$$

where u_0, v_0, w_0 are the displacements at the mid-plane in coordinate directions. To overcame the limitations of the CLPT, Reissner (1945) and Hindiin (1951) used the transverse shear strain and introduced the first order shear deformation theory (FSDT). According to FSDT, displacement fields are given as:

$$\begin{aligned} u(x,y,\mathrm{z}) &= u_0(x,y) + \mathrm{z}\,\theta_x \\ v(x,y,\mathrm{z}) &= v_0(x,y) + \mathrm{z}\,\theta_y \\ w(x,y,\mathrm{z}) &= w_0(x,y) \end{aligned} \tag{2.2}$$

where θ_x, θ_y are the rotations about x and y axis respectively. FSDT require the shear correction factor to influence transverse shear stress at top and bottom surface equivalent to zero which

was the challenging task. Both CLPT and FSDT give great outcomes for thin plates but fail in case of thick plates. This assists the advancement of higher order shear deformation theory (HSDT).

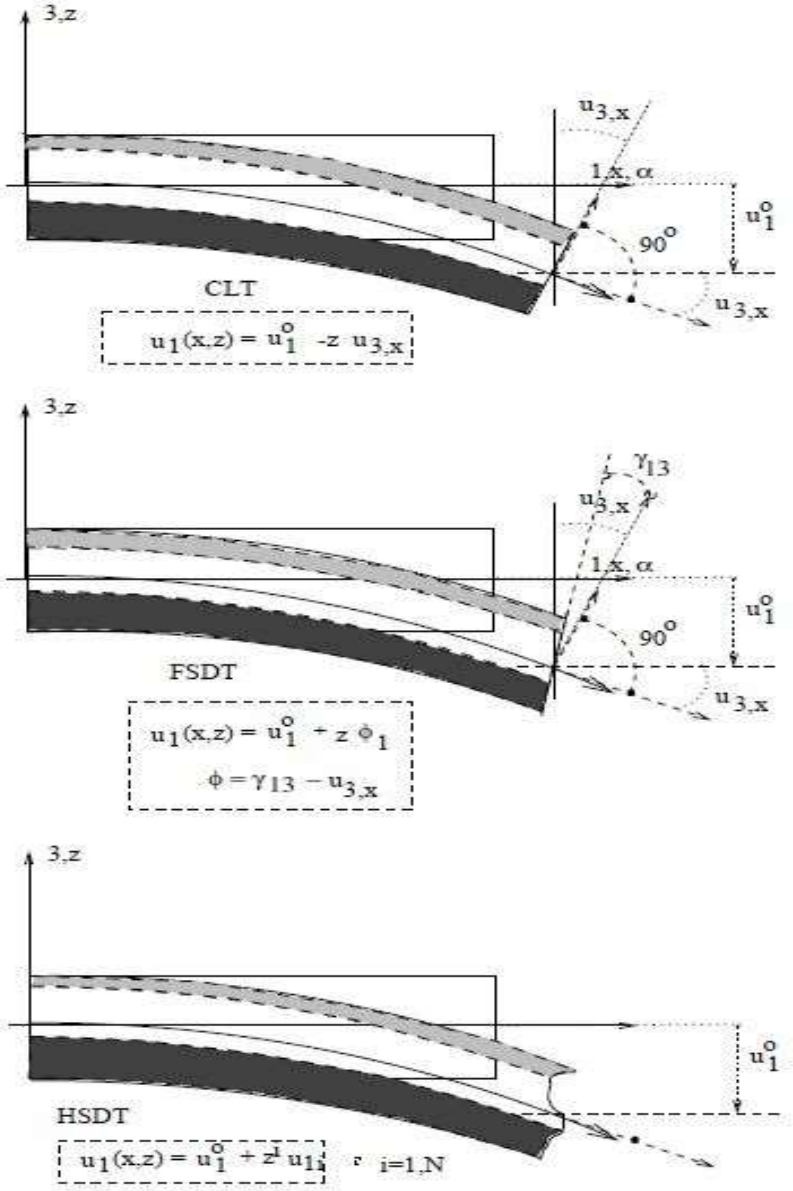

Figure 2.1 CLT, FSDT and HSDT for one-dimensional case [Carrera,2002]

HSDT is further classified into two theories as follows:

1. Polynomial Shear Deformation Theories

Polynomial shear deformation theories eliminate the requirement for shear correction factor as the impacts of transverse shear strain initiated with the assistance of polynomial coefficients of higher order terms in the Taylor series expansion.

Murthy (1981) developed a polynomial higher order shear deformation theory to study the bending behavior of the laminated and isotropic plates.

Reddy (1984) proposed a polynomial higher order shear deformation theory for the laminated composite plates. The outcomes were contrasted with the three-dimensional elasticity solutions and first order shear deformations theory solutions. The developed theory anticipates the deflections and stresses more accurately.

Kant *et al.* (1988) developed the polynomial shear deformation C^0 continuous finite element to inspect the transient response of isotropic, orthotropic and layered anisotropic composite plates. Numerical results were obtained for deflections and stresses under various boundary conditions and compared with available literature.

2. Non-polynomial Shear Deformation Theories

Non-polynomial shear deformation theories utilize the non-polynomial function which fulfills the condition for zero transverse shear stress at the top and bottom surface without help of shear correction factor.

Aydogdu (2009) presented a higher order non-polynomial shear deformation theory having exponential function and obtained the results of bending, free vibration and buckling response for simply supported composite plates under transverse load.

Mieche *et al.* (2011) studied the thick functionally graded sandwich plates for analysis of free vibration and buckling response by introducing a new hyperbolic shear deformation theory. The results obtained for plate with differing proportion of thickness utilizing the developed theory were more accurate than the results of classical plate theory but are almost comparable to the results of higher order theories having higher number of unknowns.

Mantari *et al.* (2012) developed a shear deformation theory based on trigonometric function and obtained the results for the vibrational as well as static response of the sandwich and laminated plates.

Belabed *et al.* (2014) presented a hyperbolic higher shear deformation theory for functionally graded plates. Equation of motion were obtained using Hamilton's principle. The comparison

of the obtained analytical results is done with 3-D and quasi-3-D solutions and observed the accurate results for the same.

2.3 Analysis of Functionally Graded Materials

Functionally Graded Material (FGM) are heterogeneous composite material, first introduced in 1984 as ultra-high temperature resistant materials for aircraft, space vehicles and other engineering applications by a group of material scientist in Japan. In engineering, the most commonly used structural component is rotating disc in many engineering applications such as steam and gas turbine rotors, flywheels, turbo generators, automotive brakes, ship propellers, gears and sprockets, pulleys, pump impellors, fans [Khanna *et al.* (2015,2017)].

Feldman and Aboudi (1997) studied the behavior of buckling for functionally graded plates subjected to uniaxial loading. The method used was based on the combination of micro-mechanical and structural approach, whereas two approaches were used for modeling for FGM i.e. homogenization of FGM and coupling between microstructural and global macrostructural.

Woo and Meguid (2001) discussed the non-linear analysis of functionally graded plates and shallow shells. They provided analytic solution for the coupled large deflection under transverse mechanical load and temperature field, using power law. The fundamental equations were derived from Von-Karman theory for large transverse deflection and the solution is obtained in the terms of Fourier series. It was found that the thermo-mechanical coupling effect plays a major role in dictating the response of FGM Shell.

Su and Hwan (2004) performed three-dimensional thermal buckling analysis of functionally graded materials modelled using power law. They considered 18-node solid element was considered for finite element method to analyze the variation of temperature and material properties over a thickness domain. Thermal buckling behavior under non-uniform and uniform temperature rise was obtained. The effects of temperature, volume fraction and system geometric parameters on the critical buckling temperature were also examined. And it was observed that the mentioned parameters influence the functionally graded materials significantly.

Ho and Ling (2006) discussed both closed form solution exemplified by Fourier series expression as well as finite element solutions for an elastic, rectangular and simply supported

functionally graded material plate whose properties vary according to power (P), sigmoid (S) and exponential (E) law. The analytical solutions of P-, S- and E-FGM plates were demonstrated by the numerical results of FEM. The results showed that the formulation of the solutions for FGM plates and homogeneous plates were similar but the bending stiffness expression for FGM plates were more complicated than homogeneous plates.

Najafizadeh and Heydari (2008) carried out the buckling of Functionally Graded Circular Plates (FGCP) under radial compression. The equilibrium and stability equations of FGCP were obtained from HSDT. The results obtained are compared with the FSDT and CPT. They reasoned that HSDT predicts accurate outcomes for FGCP precisely though FSDT and CPT overestimates the buckling load.

Bagherizadeh *et al.* (2011) studied the mechanical buckling of FGM cylindrical shells subjected to combined axial and radial compressive loads is embedded in an outer elastic medium. The material properties of FGM cylindrical shell varied as per the power law across thickness dimension. The two parameter Pasternak model was acquired by adding shear layer to Winkler model to use to modelled an elastic foundation. And investigated the impacts of shell geometry and the volume fraction exponent on the critical buckling load. The numerical results demonstrate the significant effect of elastic foundation on the critical buckling load.

Meiche *et al*. (2011) proposed the new hyperbolic shear deformation for buckling and free vibration analysis of thick functionally graded sandwich plate by taking transverse shear deformation effects. Unlike other theories it only gives four governing equations, four unknown variables and equation of motions were obtained using Hamilton's principle. Naiver solution was being used to solve the analytical method. The result of this theory was more accurate than the results of classical plate theory and many more higher order shear deformation theories having many numbers of unknown variables.

Sofiyeh and Kuruoglu (2014) discussed the functionally graded orthotropic cylindrical shells under external pressure for analyzing the buckling and vibration of shear deformable using Shear Deformation Theory. Basic equation used were derived using Donnell Shell Theory and solved using Galerkin Theory.

Thai *et al.* (2014) presented the new first-order shear deformation theory for functionally graded sandwich plates composed of functionally graded face sheets and an isotropic homogeneous core. The shear correction factor was not required as the transverse shear stresses were directly assessed from the transverse shear forces by utilizing equilibrium equations. Results were compared with that of present first-order shear deformation theory and higher order shear deformation theory with more number of unknowns and the obtained results were more exact than the existed theories.

Grover *et al.* (2014) performed the analysis of structural response using ITSDT developed by them on composite and sandwich plates. Numerical analysis was done to study the effects of various parameters.

Kulkarni *et al*. (2015) employed the inverse trigonometric shear deformation theory originally developed by Grover *et al.* (2013) for laminated composite shells to analyze the bending and buckling analysis on functionally graded plates. Bending analysis comprised determines in-plane and transverse displacement along with the in-plane and transverse normal and shear stresses. Calculations of critical buckling is comprised in buckling analysis. Also, studied the effect of power index, aspect ratio, span-thickness ratio, in-plane loading on buckling and bending.

Liu *et al.* (2016) discussed a layer-wise shear deformation theory and discretized with a differential quadrature finite element method (DQFEM) for functionally graded sandwich shells and laminated composite shells. This approach estimated the field variables accurately even when compared to other results based on layer-wise theories. Effective material properties of the FGM were evaluated according to two micro-mechanical models, namely, Voigt's rule of mixture (ROM) and Mori-Tanaka (MT) scheme.

Meksi *et al.* (2017) introduced a new shear deformation theory to illustrate the bending, buckling and free vibration response of FGM sandwich plates includes four unknowns. Navier solution is used to determine analytical solution for simply supported rectangular sandwich plates. Additionally, considered numerical technique for the effect of critical buckling loads, deflections, stresses, characteristic frequencies and sandwich plate type on the bending, buckling and free vibration responses of FG sandwich plates.

Joshan *et al.* (2017) investigated the thermo-mechanical response of cross-ply and angle-ply laminated composite plates. Results are generated and compared with the existing results for various examples. The applicability and accuracy of IHSDT for thermo-mechanical is ascertained.

Joshan *et al.* (2017) developed a new polynomial theory for hygro-thermo-mechanical response of laminated composite plates. Variety of examples are considered in order to evaluate the capability of the present model.

2.4 Gaps in Literature

- It is observed that the shear deformation theory based on inverse hyperbolic (IHSDT) has not been implemented for FG shells.
- It is also identified that the analysis of buckling response on the FGM shells is limited in the available literature.
- The analytical and finite element method was used for functionally graded plates but not much discussed for functionally graded shells for the buckling response.

2.5 Problem Formulation

The objective is set after the survey of the literature for present work is as follows:

- Mathematical Modelling of the Functionally Graded Shells using IHSDT
- Buckling Analysis of Functionally Graded doubly curved spherical and cylindrical shells
- Study of buckling behavior of FG doubly curved spherical and cylindrical shells using closed form solution
- Buckling analysis and modeling of FG doubly curved spherical and cylindrical shells using Finite Element Method

Summary

The literature survey is focused on the development of the theories for the analysis of the materials. It is focused on the modelling and the solution methodology for the FGM cylindrical and spherical shells. The problem is formulated on the basis of gaps identified during the review of literature.

CHAPTER 3 MATHEMATICAL FORMULATION

3.1 Introduction

The following section presents the formulation for modelling of the functionally graded doubly curved spherical and cylindrical shells are subjected to buckling load. The theory for analyzing the FGM shells is Inverse Hyperbolic Shear Deformation Theory [Grover *et al.* (2013)]. The analysis is carried out using two different approaches one is analytical and other is numerical method. For analytical solution, governing differential equations are generated using principle of virtual work and Navier exact solution method is used to satisfy the boundary conditions. The strain energy due to linear and non-linear strains are considered in finite element method for analysis of buckling response.

The doubly curved shell as shown in Figure 3.1 having dimension *a* x *b* x *h*, where '*a*' is the length, '*b*' is the width and '*h*' is the thickness of the shell. R_1 and R_2 are radii of normal curvature of mid-surface; if they tend to go to infinity the shell converts to the plate. The ξ_1 and ξ_2 curves are lines of shell mid surface, while ξ_3 is a straight line normal to the mid-surface. The gradation of the FGM material properties depends on the power law or exponential law.

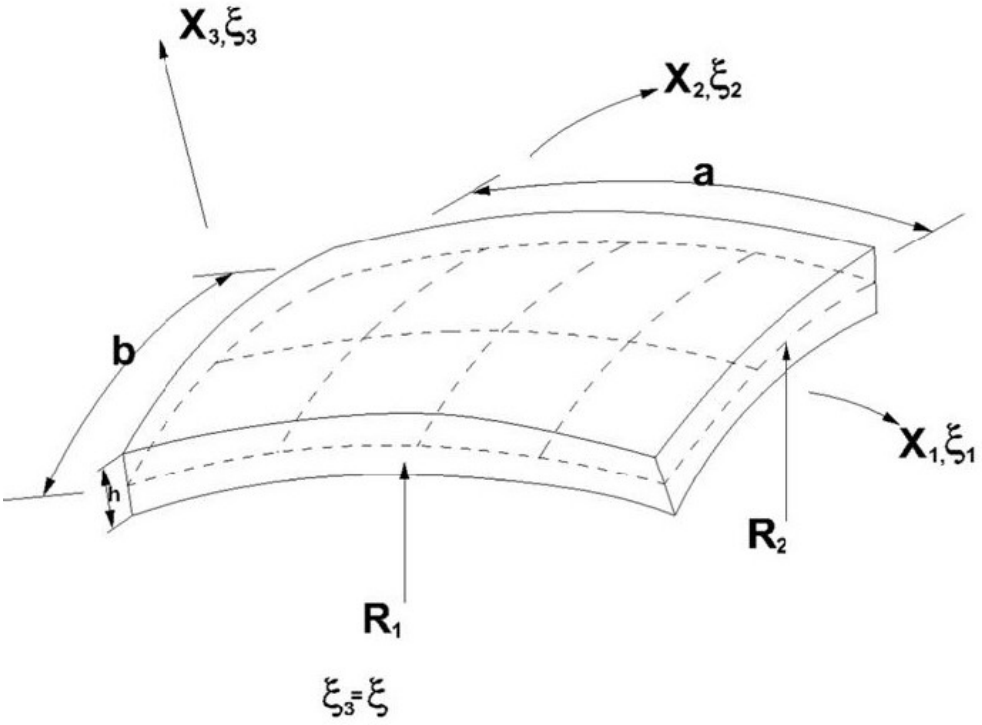

Figure 3.1 Doubly curved shells with cartesian and curvilinear co-ordinates [Oktem *et al.* (2012)]

3.2 Material Gradation Laws

As already discussed that the properties of functionally graded material changes continuously over the thickness dimension. The gradation in the properties has been assumed according to the two different laws i.e. Power law and Exponential law, discussed as follows:

(a) Power Law

The arithmetic average of constituent properties is the effective property of the FGM and is given by

$$E_e = E_m + (E_c - E_m) v_c(\xi_3) \tag{3.1}$$

where E_m and E_c represent the properties of Young's modulus of metal and ceramic respectively, and $v_c(\xi_3)$ represents the volume fraction of ceramic altered with respect to thickness coordinate (ξ_3) according to the following law

$$v_c(\xi_3) = (\xi_3/h + 1/2)^N \tag{3.2}$$

The value of N (power index) varies from zero to infinity where $N=0$ represents a shell made up of ceramic phase only and $N=\infty$ represents a shell made up of metal phase only [Kulkarni *et al*., 2015]. Figure 3.2 demonstrates the variety in the volume fraction across the thickness for various values of the power index.

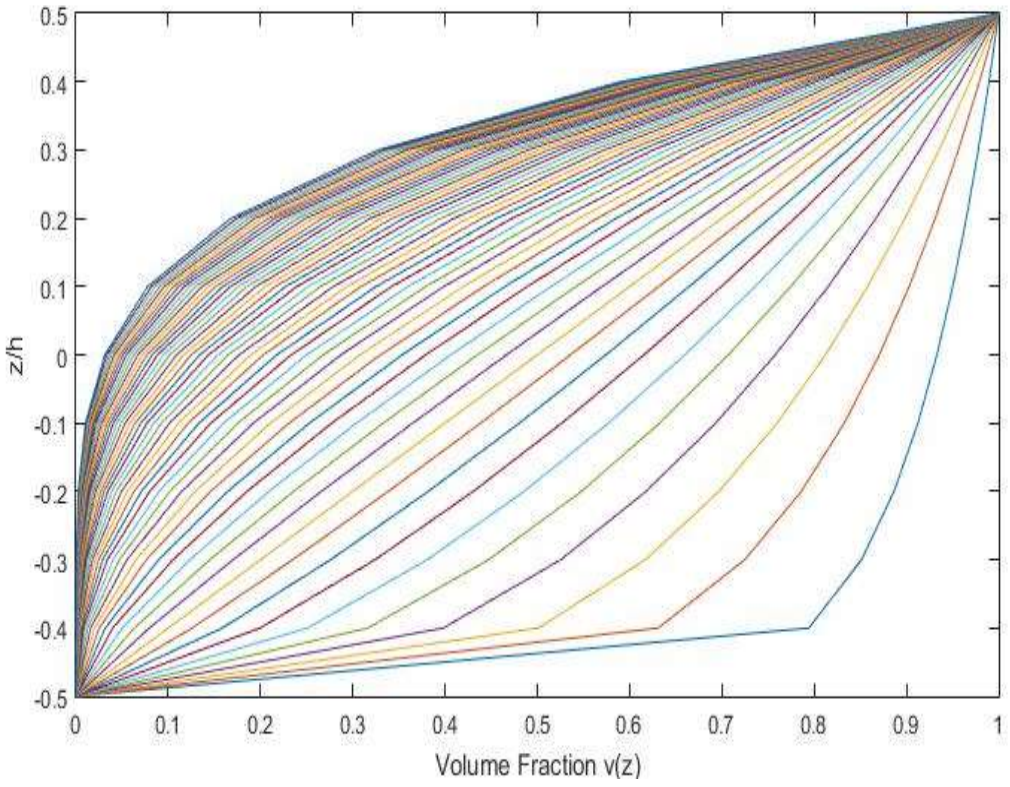

Figure 3.2 Variation of volume fraction according to power law

(b) Exponential Law

The properties of the material changes from bottom to top across any dimension (ξ_3). According to the exponential law, the expression is given by [Kulkarni *et al*., 2015]:

$$E_e = E_0 e^{N\left(z+\frac{1}{2}\right)} \tag{3.3}$$

Where E_e is effective property of the material across the dimension (ξ_3) . E_0 is the property of the bottom surface equals to the property of the metal (E_m). N represents power index according to which the total variation of the property is taking place. Figure 3.3 indicates the change in the properties of material for different values of power index, in accordance with the exponential law.

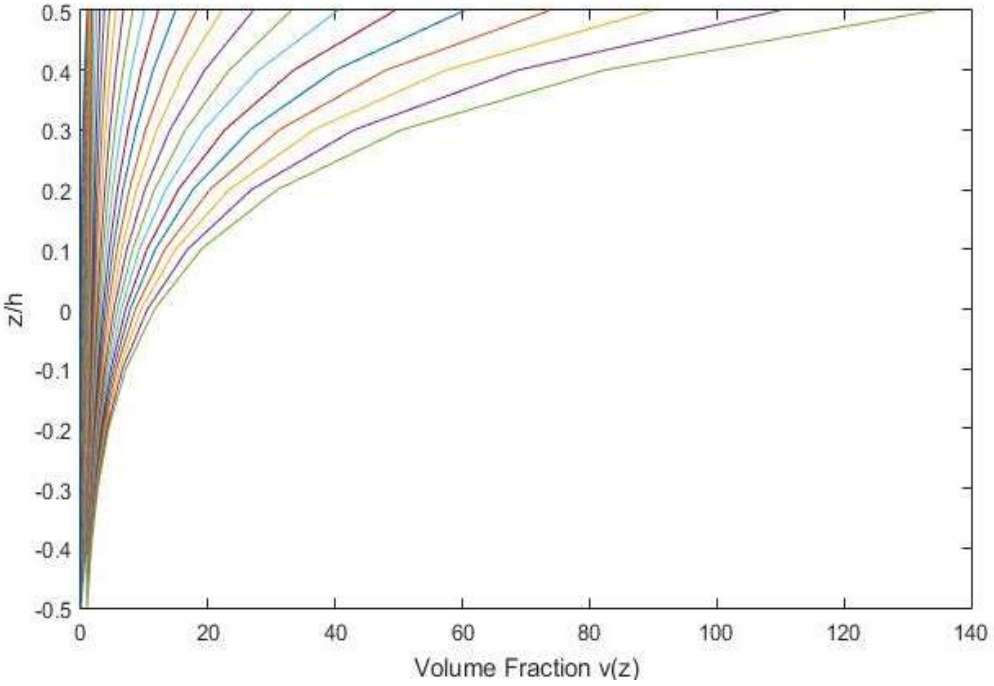

Figure 3.3 Variation in volume fraction by exponential law

3.3 Generalized Displacements

A Shells of thickness (*h*) is considered and the generalized displacement field for shell is presented by the following equation [Mantari *et al.* (2012)]:

$$\begin{aligned}
u(\xi_1,\xi_2,\xi_3) &= \left(1+\frac{\xi_3}{R_1}\right)u_0 + \xi_3\left[\Omega\phi_1 - \frac{\partial w_0}{a_1\partial\xi_1}\right] + f(\xi_3)\phi_1 \\
v(\xi_1,\xi_2,\xi_3) &= \left(1+\frac{\xi_3}{R_2}\right)v_0 + \xi_3\left[\Omega\phi_2 - \frac{\partial w_0}{a_2\partial\xi_2}\right] + f(\xi_3)\phi_2 \\
w(\xi_1,\xi_2,\xi_3) &= w_0
\end{aligned} \tag{3.4}$$

where u_0, v_0, w_0, ϕ_1 and ϕ_2 are the five unknown displacement functions at the middle surface of the panel. The function is given as [Grover *et al.* (2013)]:

$$f(\xi_3) = g(\xi_3) + \Omega\xi_3 \quad \text{such that} \quad g(\xi_3) = \sinh^{-1}(r\xi_3/h) \text{ and } \Omega = \left(-2r/h\sqrt{r^2+4}\right) \tag{3.5}$$

Where $g(\xi_3)$ is inverse hyperbolic function of ξ_3 and Ω is a constant. The parameter r is taken as 3. The value of Ω is considered in such a way that there is no need of shear correction factor and it satisfies the transverse shear conditions.

3.4 Strain Displacement Relation

The strain-displacement relation in terms of displacement fields are used given as under the assumption of small displacements and rotations:

$$\begin{aligned}
\varepsilon_1 &= \frac{1}{A_1}\left(\frac{\partial u}{\partial \xi_1} + \frac{1}{a_2}\frac{\partial a_1}{\partial \xi_2}v + \frac{a_1}{R_1}w\right) \\
\varepsilon_2 &= \frac{1}{A_2}\left(\frac{\partial v}{\partial \xi_2} + \frac{1}{a_1}\frac{\partial a_2}{\partial \xi_1}u + \frac{a_2}{R_2}w\right) \\
\varepsilon_4 &= \frac{1}{A_2}\frac{\partial w}{\partial \xi_2} + A_2\frac{\partial}{\partial \xi_3}\left(\frac{v}{A_2}\right) \\
\varepsilon_5 &= \frac{1}{A_1}\frac{\partial w}{\partial \xi_1} + A_1\frac{\partial}{\partial \xi_3}\left(\frac{u}{A_1}\right) \\
\varepsilon_6 &= \frac{A_2}{A_1}\frac{\partial}{\partial \xi_1}\left(\frac{v}{A_2}\right) + \frac{A_1}{A_2}\frac{\partial}{\partial \xi_2}\left(\frac{u}{A_1}\right)
\end{aligned} \tag{3.6}$$

where

$$A_1 = \left(1 + \frac{\xi_3}{R_1}\right)a_1;\ A_2 = \left(1 + \frac{\xi_3}{R_2}\right)a_2 \tag{3.7}$$

After generalizing, displacements are put in strain displacement relation and differentiated to get the following equations [Mantari *et al*. (2012)]:

$$\begin{aligned}
\varepsilon_1 &= \varepsilon_1^0 + \xi_3\varepsilon_1^1 + f(\xi_3)\varepsilon_1^2 \\
\varepsilon_2 &= \varepsilon_2^0 + \xi_3\varepsilon_2^1 + f(\xi_3)\varepsilon_2^2 \\
\varepsilon_6 &= \varepsilon_6^0 + \xi_3\varepsilon_6^1 + f(\xi_3)\varepsilon_6^2 \\
\varepsilon_4 &= \Omega\varepsilon_4^0 + f'(\xi_3)\varepsilon_4^3 \\
\varepsilon_5 &= \Omega\varepsilon_5^0 + f'(\xi_3)\varepsilon_5^3
\end{aligned} \tag{3.8}$$

where

$$\varepsilon_1^0 = \frac{\partial u}{\partial x_1} + \frac{w}{R_1}, \varepsilon_1^1 = \Omega \frac{\partial \phi_1}{\partial x_1} - \frac{\partial^2 w}{\partial x_2^2}, \varepsilon_1^2 = \frac{\partial \phi_1}{\partial x_1}$$

$$\varepsilon_2^0 = \frac{\partial v}{\partial x_2} + \frac{w}{R_2}, \varepsilon_2^1 = \Omega \frac{\partial \phi_2}{\partial x_2} - \frac{\partial^2 w}{\partial x_2^2}, \varepsilon_2^2 = \frac{\partial \phi_2}{\partial x_2}$$

$$\varepsilon_6^0 = \frac{\partial v}{\partial x_1} + \frac{\partial u}{\partial x_2}, \varepsilon_6^1 = \Omega \frac{\partial \phi_2}{\partial x_1} + \Omega \frac{\partial \phi_1}{\partial x_2} - 2\frac{\partial^2 w}{\partial x_1 \partial x_2}, \varepsilon_6^2 = \frac{\partial \phi_2}{\partial x_1} + \frac{\partial \phi_1}{\partial x_2} \tag{3.9}$$

$$\varepsilon_4^0 = \phi_2, \varepsilon_4^3 = \phi_2$$

$$\varepsilon_5^0 = \phi_1, \varepsilon_5^3 = \phi_1$$

where x_i refers to the cartesian coordinate $dx_i = a_i d\xi_i, i = 1,2$

3.5 Stress-Strain Relation

The stress strain relation for FG shell is stated as:

$$\begin{Bmatrix} \sigma_1 \\ \sigma_2 \\ \sigma_4 \\ \sigma_5 \\ \sigma_6 \end{Bmatrix} = \begin{bmatrix} Q_{11} & Q_{12} & 0 & 0 & 0 \\ Q_{21} & Q_{22} & 0 & 0 & 0 \\ 0 & 0 & Q_{44} & 0 & 0 \\ 0 & 0 & 0 & Q_{55} & 0 \\ 0 & 0 & 0 & 0 & Q_{66} \end{bmatrix} \begin{Bmatrix} \varepsilon_1 \\ \varepsilon_2 \\ \varepsilon_4 \\ \varepsilon_5 \\ \varepsilon_6 \end{Bmatrix} \tag{3.10}$$

where (σ_1, σ_2, σ_6, σ_4, σ_5) are stress and (ε_1, ε_2, ε_6, ε_4, ε_5) are strain components and Q_{ij} (i=1,2,6,4,5) are the material constant which depends on the material properties such as Poisson's ratio, Young's modulus and Shear modulus. [Kulkarni *et al*., 2015]

$$Q_{11} = Q_{22} = \frac{E(\xi_3)}{1-\nu^2}; Q_{12} = Q_{22} = \frac{\nu E(\xi_3)}{1-\nu^2};$$
$$Q_{44} = Q_{55} = Q_{66} = \frac{E(\xi_3)}{2(1+\nu)} \tag{3.11}$$

3.6 Governing Differential Equations

The governing differential equations for analysis under in-plane load obtained by using Principle of Virtual Work is given as:

$$\int_0^T (\delta U - \delta V)\, dt = 0 \tag{3.12}$$

where virtual strain energy, δU and virtual work done by applied forces, δV are given as:

$$0 = \int_{-h/2}^{h/2} \left\{ \int_\Omega^{(k)} \left[\sigma_1 \delta\varepsilon_1^{(k)} + \sigma_2 \delta\varepsilon_2^{(k)} + \sigma_6 \delta\varepsilon_6^{(k)} + \sigma_4 \delta\varepsilon_4^{(k)} + \sigma_5 \delta\varepsilon_5^{(k)} \right] dx_1 dx_2 \right\} d\xi_3 \tag{3.13}$$

Virtual strains are expressed in terms of displacement field and by integrating them by parts. We get the governing differential equations in terms of resultant stress and moments as expressed by:

$$\frac{\partial N_1}{\partial x_1}+\frac{\partial N_6}{\partial x_2}=0$$

$$\frac{\partial N_2}{\partial x_2}+\frac{\partial N_6}{\partial x_1}=0$$

$$-\frac{N_1}{R_1}-\frac{N_2}{R_2}+\frac{\partial^2 M_1}{\partial x_1^2}+\frac{\partial^2 M_2}{\partial x_2^2}+2\frac{\partial^2 M_6}{\partial x_1 \partial x_2}+\overline{N}_{xx}\frac{\partial^2 w_0}{\partial {x_1}^2}+2\overline{N}_{xy}\frac{\partial^2 w_0}{\partial x_1 \partial x_2}+\overline{N}_{yy}\frac{\partial w_0}{\partial x_1}=0 \qquad (3.14)$$

$$\frac{\partial P_1}{\partial x_1}+\frac{\partial P_6}{\partial x_2}+\Omega\frac{\partial M_1}{\partial x_1}+\Omega\frac{\partial M_6}{\partial x_2}-Q_1-K_1=0$$

$$\frac{\partial P_2}{\partial x_2}+\frac{\partial P_6}{\partial x_1}+\Omega\frac{\partial M_2}{\partial x_2}+\Omega\frac{\partial M_6}{\partial x_1}-Q_2-K_2=0$$

where resultant stresses and moments are as follows

$$\begin{bmatrix} N_1 & M_1 & P_1 \\ N_2 & M_2 & P_2 \\ N_6 & M_6 & P_6 \end{bmatrix}=\int_{-h/2}^{h/2}\begin{Bmatrix}\sigma_1\\ \sigma_2\\ \sigma_6\end{Bmatrix}\begin{bmatrix}1 & \xi_3 & f(\xi_3)\end{bmatrix}d\xi_3$$

$$\begin{bmatrix} Q_1 & K_1 \\ Q_2 & K_2 \end{bmatrix}=\int_{-h/2}^{h/2}\begin{Bmatrix}\sigma_5\\ \sigma_4\end{Bmatrix}\begin{bmatrix}1 & f'(\xi_3)\end{bmatrix}d\xi_3 \qquad (3.15)$$

$$\begin{bmatrix}A_{ij} & B_{ij} & D_{ij} & E_{ij} & F_{ij} & H_{ij}\end{bmatrix}=\int_{-h/2}^{h/2}\begin{bmatrix}Q_{ij}^{(k)}\end{bmatrix}\begin{bmatrix}1 & \xi_3 & \xi_3^2 & g(\xi_3) & \xi_3 g(\xi_3) & (g(\xi_3))^2\end{bmatrix}d\xi_3$$

For *i, j*=1, 2, 4, 5, 6

$$\begin{bmatrix}K_{ij} & L_{ij}\end{bmatrix}=\int_{-h/2}^{h/2}\begin{bmatrix}Q_{ij}^{(k)}\end{bmatrix}_{2x2}\begin{bmatrix}g'(\xi_3) & (g'(\xi_3))^2\end{bmatrix}d\xi_3 \text{ for i, j=4, 5}$$

By solving the above equation by integrating, the governing equation can be derived from principle of virtual work. Equations 3.10a-e are coefficients of δu_0, δv_0, δw_0, $\delta\phi_1$ and $\delta\phi_2$ [Mantari *et al*., 2012].

The following are the stiffness coefficients which are equal to zero expressed as:

$A_{i6} = B_{i6} = D_{i6} = E_{i6} = F_{i6} = H_{i6} = 0$, (i = 1, 2)

$A_{45} = K_{45} = L_{45} = 0$

$$A_{11}\left(\frac{\partial^2 u}{\partial x_1^2}+\frac{1}{R_1}\frac{\partial w}{\partial x_1}\right)+B_{11}\left(\Omega\frac{\partial^2\phi_1}{\partial x_1^2}-\frac{\partial^3 w}{\partial x_1^3}\right)+E_{11}\left(\frac{\partial^2\phi_1}{\partial x_1^2}\right)+A_{12}\left(\frac{\partial^2 v}{\partial x_1\partial x_2}+\frac{1}{R_2}\frac{\partial w}{\partial x_1}\right)$$
$$+B_{12}\left(\Omega\frac{\partial^2\phi_2}{\partial x_1\partial x_2}-\frac{\partial^3 w}{\partial x_1\partial x_2^2}\right)+E_{12}\left(\frac{\partial^2\phi_2}{\partial x_1\partial x_2}\right)+A_{66}\left(\frac{\partial^2 v}{\partial x_1\partial x_2}+\frac{\partial^2 u}{\partial x_2^2}\right)$$
$$+B_{66}\left[\Omega\left(\frac{\partial^2\phi_2}{\partial x_1\partial x_2}+\frac{\partial^2\phi_1}{\partial x_2^2}\right)-2\frac{\partial^3 w}{\partial x_1\partial x_2^2}\right]+E_{66}\left(\frac{\partial^2\phi_2}{\partial x_1\partial x_2}+\frac{\partial^2\phi_1}{\partial x_2}\right)=0$$

$$A_{21}\left(\frac{\partial^2 u}{\partial x_1 \partial x_2}+\frac{1}{R_1}\frac{\partial w}{\partial x_2}\right)+B_{21}\left(\Omega\frac{\partial^2 \phi_1}{\partial x_1 \partial x_2}-\frac{\partial^3 w}{\partial x_1^2 \partial x_2}\right)+E_{21}\left(\frac{\partial^2 \phi_2}{\partial x_2^2}\right)+A_{22}\left(\frac{\partial^2 v}{\partial x_2^2}+\frac{1}{R_2}\frac{\partial w}{\partial x_2}\right)$$
$$+B_{22}\left(\Omega\frac{\partial^2 \phi_2}{\partial x_2^2}-\frac{\partial^3 w}{\partial x_2^3}\right)+E_{22}\left(\frac{\partial^2 \phi_2}{\partial x_2^2}\right)+A_{66}\left(\frac{\partial^2 v}{\partial x_1^2}+\frac{\partial^2 u}{\partial x_1 \partial x_2}\right)$$
$$+B_{66}\left[\Omega\left(\frac{\partial^2 \phi_2}{\partial x_1^2}+\frac{\partial^2 \phi_1}{\partial x_1 \partial x_2}\right)-2\frac{\partial^3 w}{\partial x_1^2 \partial x_2}\right]+E_{66}\left(\frac{\partial^2 \phi_2}{\partial x_1^2}+\frac{\partial^2 \phi_1}{\partial x_1 \partial x_2}\right)=0$$

$$-\frac{1}{R_1}\left[\begin{array}{l}A_{11}\left(\frac{\partial u}{\partial x_1}+\frac{w}{R_1}\right)+B_{11}\left(\Omega\frac{\partial \phi_1}{\partial x_1}-\frac{\partial^2 w}{\partial x_1^2}\right)+E_{11}\left(\frac{\partial \phi_1}{\partial x_1}\right)\\ +A_{12}\left(\frac{\partial v}{\partial x_2}+\frac{w}{R_2}\right)+B_{12}\left(\Omega\frac{\partial \phi_2}{\partial x_2}-\frac{\partial^2 w}{\partial x_2^2}\right)+E_{12}\left(\frac{\partial \phi_2}{\partial x_2}\right)\end{array}\right]-\frac{N_2}{R_2}+\frac{\partial^2 M_1}{\partial x_1^2}$$
$$+\frac{\partial^2 M_2}{\partial x_2^2}+2\frac{\partial^2 M_6}{\partial x_1 \partial x_2}+q=0 \qquad (3.16)$$

$$E_{11}\left(\frac{\partial^2 u}{\partial x_1^2}+\frac{1}{R_1}\frac{\partial w}{\partial x_1}\right)+F_{11}\left(\Omega\frac{\partial^2 \phi_1}{\partial x_2^2}-\frac{\partial^3 w}{\partial x_1^3}\right)+H_{11}\left(\frac{\partial^2 \phi_1}{\partial x_1^2}\right)+E_{12}\left(\frac{\partial^2 v}{\partial x_1 \partial x_2}+\frac{1}{R_2}\frac{\partial w}{\partial x_1}\right)$$
$$+F_{12}\left(\Omega\frac{\partial^2 \phi_2}{\partial x_1 \partial x_2}-\frac{\partial^3 w}{\partial x_1 \partial x_2^2}\right)+H_{12}\left(\frac{\partial^2 \phi_2}{\partial x_1 \partial x_2}\right)+\frac{\partial P_6}{\partial x_2}+\Omega\left(\frac{\partial M_1}{\partial x_1}+\frac{\partial M_6}{\partial x_2}\right)-Q_1-K_1=0$$

$$E_{21}\left(\frac{\partial^2 u}{\partial x_1 \partial x_2}+\frac{1}{R_1}\frac{\partial w}{\partial x_2}\right)+F_{21}\left(\Omega\frac{\partial^2 \phi_1}{\partial x_1 \partial x_2}-\frac{\partial^3 w}{\partial x_1^2 \partial x_2}\right)+H_{21}\left(\frac{\partial^2 \phi_2}{\partial x_2^2}\right)+E_{22}\left(\frac{\partial^2 v}{\partial x_2^2}+\frac{1}{R_2}\frac{\partial w}{\partial x_2}\right)$$
$$+F_{22}\left(\Omega\frac{\partial^2 \phi_2}{\partial x_2^2}-\frac{\partial^3 w}{\partial x_2^3}\right)+H_{22}\left(\frac{\partial^2 \phi_2}{\partial x_2^2}\right)+\frac{\partial P_6}{\partial x_1}+\Omega\left(\frac{\partial M_2}{\partial x_2}+\frac{\partial M_6}{\partial x_1}\right)-Q_2-K_2=0$$

3.7 Solution Methodology

Navier type solution is being derived under the following boundary conditions [Grover *et al*. (2013)]:

$v_0 = w_0 = \phi_2 = 0$ at x=0, a

$u_0 = w_0 = \phi_1 = 0$ at y=0, b

These boundary conditions are satisfied if:

$$
\begin{aligned}
u_0 &= \sum_{m=1}^{\infty}\sum_{n=1}^{\infty} U_{mn}\cos(\alpha x)\sin(\beta y)\\
v_0 &= \sum_{m=1}^{\infty}\sum_{n=1}^{\infty} V_{mn}\sin(\alpha x)\cos(\beta y)\\
w_0 &= \sum_{m=1}^{\infty}\sum_{n=1}^{\infty} W_{mn}\sin(\alpha x)\sin(\beta y)\\
\phi_1 &= \sum_{m=1}^{\infty}\sum_{n=1}^{\infty} X_{mn}\cos(\alpha x)\sin(\beta y)\\
\phi_2 &= \sum_{m=1}^{\infty}\sum_{n=1}^{\infty} Y_{mn}\sin(\alpha x)\cos(\beta y)\\
\alpha &= \frac{m\pi}{a}, \beta = \frac{n\pi}{b}
\end{aligned}
\tag{3.17}
$$

For simplification of the equations the five equations with five unknown arbitrary parameters (U_{mn}, V_{mn}, W_{mn}, X_{mn}, and Y_{mn}) are there which can solve by any suitable numerical method. The buckling response of functionally graded shells are evaluated by the in-plane compression that might be uniaxial, biaxial and unequal biaxial loads. For uniaxial the value will be k=0; for biaxial, k=1 and for the unequal biaxial load k>1. The generalized of governing differential equations for buckling is given as:

$$
\left[\overline{R}\right] - \lambda^2\left[G\right]\{\Delta\} = \{0\} \tag{3.18}
$$

where $\overline{R}$ is the stiffness coefficient matrix mentioned in Appendix A and G is the matrix of in-plane load. Above equation is solved using eigenvalue and is solved for critical buckling load.

3.8 Finite Element Method for Analysis of FGMs Shells

The closed form solutions have limitations regarding boundary conditions that is it only give results for simply supported boundary conditions. Thus, the functionally graded doubly curved spherical as well as cylindrical shells are considered for modelled using numerical method that is finite element method. It gives the liability to get results for different boundary conditions.

3.8.1 Displacement Fields

Displacement field for FGM shells is presented by the following equation:

$$
\begin{aligned}
u(\xi_1,\xi_2,\xi_3) &= \left(1+\frac{\xi_3}{R_1}\right)u_0 + \xi_3\left[\Omega\phi_1 - \frac{\partial w_0}{a_1\partial\xi_1}\right] + f(\xi_3)\phi_1\\
v(\xi_1,\xi_2,\xi_3) &= \left(1+\frac{\xi_3}{R_2}\right)v_0 + \xi_3\left[\Omega\phi_2 - \frac{\partial w_0}{a_2\partial\xi_2}\right] + f(\xi_3)\phi_2\\
w(\xi_1,\xi_2,\xi_3) &= w_0
\end{aligned}
\tag{3.19}
$$

The artificial constraints are introduced due to additional degree of freedom as follows:

$$\frac{\partial w_0}{\partial \xi_1} = \phi_x ; \frac{\partial w_0}{\partial \xi_2} = \phi_y \tag{3.20}$$

substituted in the displacement fields equation 3.18 and we get,

$$\begin{aligned} u(\xi_1, \xi_2, \xi_3) &= \left(1 + \frac{\xi_3}{R_1}\right) u_0 + \xi_3 \left[\Omega\theta_x - \frac{1}{a_1}\phi_x\right] + f(\xi_3)\theta_x \\ v(\xi_1, \xi_2, \xi_3) &= \left(1 + \frac{\xi_3}{R_2}\right) v_0 + \xi_3 \left[\Omega\theta_y - \frac{1}{a_2}\phi_y\right] + f(\xi_3)\theta_y \\ w(\xi_1, \xi_2, \xi_3) &= w_0 \end{aligned} \tag{3.21}$$

3.8.2 Strain-Displacement Relation

The strain-displacement relation expressed as von-Karman non-liner relations:

$$\begin{aligned} \{\varepsilon\}_{5\times1} &= \{\varepsilon_L\} + \{\varepsilon_{NL}\} \\ \{\varepsilon\}_{5\times1} &= \begin{bmatrix} \varepsilon_1 & \varepsilon_2 & \varepsilon_4 & \varepsilon_5 & \varepsilon_6 \end{bmatrix}^T \end{aligned} \tag{3.22}$$

where linear and non-linear strain are as follows:

$$\begin{aligned} \{\varepsilon_L\} &= \left[\frac{\partial u}{\partial \xi_1} \quad \frac{\partial v}{\partial \xi_2} \quad \frac{\partial u}{\partial \xi_2} + \frac{\partial v}{\partial \xi_1} \quad \frac{\partial v}{\partial \xi_3} + \frac{\partial w}{\partial \xi_2} \quad \frac{\partial u}{\partial \xi_3} + \frac{\partial w}{\partial \xi_1}\right]^T \\ \{\varepsilon_{NL}\} &= \left[\frac{1}{2}\left(\frac{\partial w}{\partial \xi_1}\right)^2 \quad \frac{1}{2}\left(\frac{\partial w}{\partial \xi_2}\right)^2 \quad \frac{1}{2}\left(\frac{\partial w}{\partial \xi_1}\right)\left(\frac{\partial w}{\partial \xi_2}\right) \quad 0 \quad 0\right]^T \end{aligned} \tag{3.23}$$

3.8.3 Element Selection

An eight-node quadrilateral element is chosen to discretize the shell geometry. The shape functions at node 'i' for eight-node element are as follows [Grover *et. al.* (2014)]:

$$N_i = \begin{cases} \frac{1}{4}(1+\xi\xi_i)(1+\eta\eta_i)(\xi\xi_i + \eta\eta_i - 1) & \text{for i=1,2,3,4} \\ \frac{1}{2}(1-\xi^2)(1+\eta\eta_i) & \text{for i=5,7} \\ \frac{1}{2}(1-\eta^2)(1+\xi\xi_i) & \text{for i=6,8} \end{cases} \tag{3.24}$$

3.8.4 Strain Energy due to Linear and Non-linear Strain

To formulate the element stiffness matrix and geometric stiffness matrix the strain energy due to linear and non-linear strains are implemented respectively. The linear strains are expressed in as:

$$\{\varepsilon_L\}_{5\times1} = [H]_{5\times13} \{\overline{\varepsilon_l}\}_{13\times1} \tag{3.25}$$

where

$$\left\{\overline{\varepsilon_l}\right\}_{13\times1}=\left\{\varepsilon_1^0 \quad \varepsilon_2^0 \quad \varepsilon_6^0 \quad \varepsilon_1^1+\Omega\varepsilon_1^2 \quad \varepsilon_2^1+\Omega\varepsilon_2^2 \quad \varepsilon_6^1+\Omega\varepsilon_6^2 \quad \varepsilon_1^1 \quad \varepsilon_2^1 \quad \varepsilon_6^1 \quad \Omega\left(\varepsilon_4^0+\varepsilon_4^3\right) \quad \Omega\left(\varepsilon_5^0+\varepsilon_5^3\right) \quad \varepsilon_4^3 \quad \varepsilon_5^3\right\}^T$$

The matrix $[H]$ and $\left\{\overline{\varepsilon_l}\right\}$ are given in the Appendix A. The generalized strains can be expressed as the field variables as:

$$\left\{\overline{\varepsilon_l}\right\}_{13\times1}=[L]_{13\times7}\{q_i\}_{7\times1} \tag{3.26}$$

where $\{q_i\}_{7\times1}=\left[u_0 \quad v_0 \quad w_0 \quad \theta_x \quad \theta_y \quad \phi_x \quad \phi_y\right]^T$

As the element strain-displacement relations for jth element can be obtained from the equations and expressed as:

$$\left\{\overline{\varepsilon_l}\right\}_{13\times1}=[B]_j\{q_i\}_j \tag{3.27}$$

The strain energy due to linear strain can be derived using equation and as follows:

$$\begin{aligned} U_i^{(j)} &= \frac{1}{2}\int_v \{\varepsilon_l\}_j^T\{\sigma\}\,dv=\frac{1}{2}\int_v \{\varepsilon_l\}_j^T\left[\overline{Q}_{ij}\right]\{\varepsilon_l\}_j\,dv=\frac{1}{2}\int_v \left\{\overline{\varepsilon_l}\right\}_j^T[H]_j^T\left[\overline{Q}_{ij}\right][H]_j\left\{\overline{\varepsilon_l}\right\}_j\,dv \\ &= \frac{1}{2}\int_s \left\{\overline{q}\right\}_j^T[B]_j^T[D]_j[B]_j\left\{\overline{q}\right\}_j\,dx\,dy=\frac{1}{2}\left\{\overline{q}\right\}_j^T[K]\left\{\overline{q}\right\}_j \end{aligned} \tag{3.28}$$

Total strain energy due to linear strain is acquired by assembling the element stiffness matrix into global stiffness matrix [*K*] given as:

$$U_l=\sum_{j=1}^{nel}U_l^{(j)}=\frac{1}{2}\{q\}^T[K]\{q\} \tag{3.29}$$

The procedure to derive strain energy due to non-linear strains is similar as strain energy due to linear strains, the obtained geometric stiffness matrix is not only depending on the geometry but also on the internal forces that exists i.e. in-plane normal stresses (S_{xx} , S_{yy}) and in-plane shear (S_{xy}). The strain energy of j^{th} element due to non-linear strain is expressed as [Grover *et. al.* (2014)]:

$$\begin{aligned} U_{nl}^{(j)} &= \frac{1}{2}\int_v \{\varepsilon_{nl}\}_j^T\{\sigma\}_j\,dv=\frac{1}{2}\int_v \{\varepsilon_{nl}\}_j^T[S]\{\varepsilon_{nl}\}_j\,dv \\ &= \frac{1}{2}\int_v \left\{\overline{\varepsilon_{nl}}\right\}_j^T\left[H_g\right]_j^T[S]\left[H_g\right]_j\left\{\overline{\varepsilon_{nl}}\right\}_j\,dv \\ &= \frac{1}{2}\int_s \left\{\overline{q}\right\}_j^T[B_G]_j^T[G]_j[B_G]_j\left\{\overline{q}\right\}_j\,dx\,dy=\frac{1}{2}\left\{\overline{q}\right\}_j^T[K_G]\left\{\overline{q}\right\}_j \end{aligned} \tag{3.30}$$

where

$$[G]=\sum_{k=1}^{nl}\int_{Z_l}^{Z_u}[H_G]^T[S][H_G]\,dz\;;\;S=\begin{bmatrix} S_{xx} & S_{xy} \\ S_{xy} & S_{yy}\end{bmatrix}$$

Assembling the elemental strain energy into global geometric stiffness matrix [K_G] as follows:

$$U_{nl} = \sum_{j=1}^{nl} U_{nl}^{(j)} = \frac{1}{2}\{q\}^T [K_G]\{q\} \tag{3.31}$$

The buckling response can be obtained by:

$$[K + \lambda K_G]\{q_i\} = \{0\} \tag{3.32}$$

where K is the stiffness matrix and K_G is the geometric stiffness matrix.

Summary

The mathematical formulation is done using IHSDT for the buckling characteristics of the FG doubly curved spherical and cylindrical shells. The formulated governing equations are done by principle of virtual work and solving them via Navier type exact solution. Also, numerical technique, Fem is done on the FG shells for buckling response.

CHAPTER 4 BUCKLING RESPONSE OF FGM SHELLS USING POWER LAW

4.1 Introduction

In this chapter, the buckling response has been studied by taking various numerical examples to demonstrate the approach discussed in the earlier chapters. Analysis of buckling load is carried for two kinds of shell i.e. singly curved or cylindrical and doubly curved or spherical. The outcome of power index, span-thickness ratio and curvature ratio is studied under uniaxial and biaxial in plane loads to know the response of the FGMs shells which are modelled using power law. The generalized MATLAB code is generated for both the methods i.e. analytical and numerical for buckling response of FGMs shells having different material properties.

The following material properties used for FGMs Shells are as follows [Kulkarni *et al.* (2013)]:

Aluminum/Alumina (Al/Al_2O_3): E_m=70GPa; E_c=380GPa; ν = 0.3

Aluminum/Zirconia (Al/ZrO_2): E_m=70GPa; E_c=168GPa; ν = 0.3

4.2 Analytical Method

FGM spherical shells are considered for the analytical simulation under in-plane loads and simply supported boundary conditions, composed of Aluminum/Alumina and Aluminum/Zirconia material properties. The closed form solution methodology is used to obtain the results. The value of transverse shear stress parameter '*r*' is optimized and taken as 3 [Grover *et al*. (2013)].

Non-dimensional buckling parameter (NDBP) is obtained by given expression:

$$\widetilde{N}_{cr} = \frac{\lambda a^2}{E_m h^3} \tag{4.1}$$

Table 4.1 shows the non-dimensional buckling parameter for FGM spherical shell composed of Aluminum/Alumina material property and also the response of FGM plate as a special case when R/a ratio goes to infinity. The comparison of results is done with the existing results given by Thai and Chou (2012), Nguyen *et al.* (2015) and Kulkarni *et al.* (2015) the present results for plates agree well with the existing results. It shows that as the power index varies when span-thickness ratio and curvature ratio remain constant, the non-dimensional buckling load decreases. It is observed that a shell with *R/a*=5 possess approximately 3.8% higher buckling load as compared to plate for *a/h*=5 while the increment in buckling load for shell with *a/h*=20 is approximately 5.4% relative to plate. Figure 4.1 shows the generated MATLAB code and as the plate is a special case of shell it also indicates the closeness of the buckling response

between the spherical shell and plate as the curvature ratio increases and tends to go to infinity. Both spherical shell and plates are made of using material properties of Aluminum/Zirconia.

Table 4.1 Non-dimensional buckling parameter of spherical shell and plate with validation under uniaxial and biaxial in-plane loads (Al/Al_2O_3)

k	a/h	N	R/a=5	R/a=20	R/a=50	R/a=∞			
			Present			Present	Thai and Chou (2012)	Nguyen *et al.* (2015)	Kulkarni *et al.* (2015)
0	5	1	8.5854	8.3412	8.2630	8.2597	8.2245	8.2597	8.2524
	10		10.6523	9.6752	9.3626	9.3496	9.3391	9.3496	9.3473
	20		14.8810	10.9729	9.7223	9.6702	9.6675	9.6702	9.6696
	5	2	6.6140	6.4258	6.3656	6.3631	6.3432	6.3631	6.3578
	10		8.2723	7.5196	7.2788	7.2687	7.2631	7.2687	7.2671
	20		11.5529	8.5422	7.5787	7.5386	7.5371	7.5386	7.5382
	5	5	5.2220	5.0569	5.0476	5.0459	5.0531	5.0459	5.0432
	10		6.7360	6.0759	6.0386	6.0316	6.0353	6.0316	6.0307
	20		9.1613	6.5198	6.3718	6.3436	6.3448	6.3437	6.3434
	5	10	4.3695	4.5063	4.4988	4.4974	4.4807	4.4981	4.4919
	10		6.0264	5.4934	5.4636	5.4579	5.4528	5.4587	5.4560
	20		8.0419	5.9103	5.7909	5.7681	5.7668	5.7689	5.7676
1	5	1	4.2927	4.1706	4.1315	4.1299	4.1122	4.1299	4.1262
	10		5.3261	4.8376	4.6813	4.6748	4.6696	4.6748	4.6737
	20		7.4405	5.4865	4.8612	4.8351	4.8337	4.8351	4.8348
	5	2	3.3070	3.2129	3.1828	3.1815	3.1716	3.1815	3.1789
	10		4.1362	3.7598	3.6394	3.6344	3.6315	3.6344	3.6336
	20		5.7764	4.2711	3.7894	3.7693	3.7686	3.7693	3.7691
	5	5	2.6110	2.5284	2.5238	2.5229	2.5265	2.5230	2.5216
	10		3.3680	3.0378	3.0193	3.0158	3.0177	3.0158	3.0154
	20		4.5807	3.2599	3.1859	3.1718	3.1724	3.1718	3.1717
	5	10	2.3198	2.2531	2.2494	2.2487	2.2403	2.2491	2.2459
	10		3.0132	2.7467	2.7318	2.729	2.7264	2.7293	2.728
	20		4.0210	2.9551	2.8954	2.8841	2.8834	2.8844	2.8838

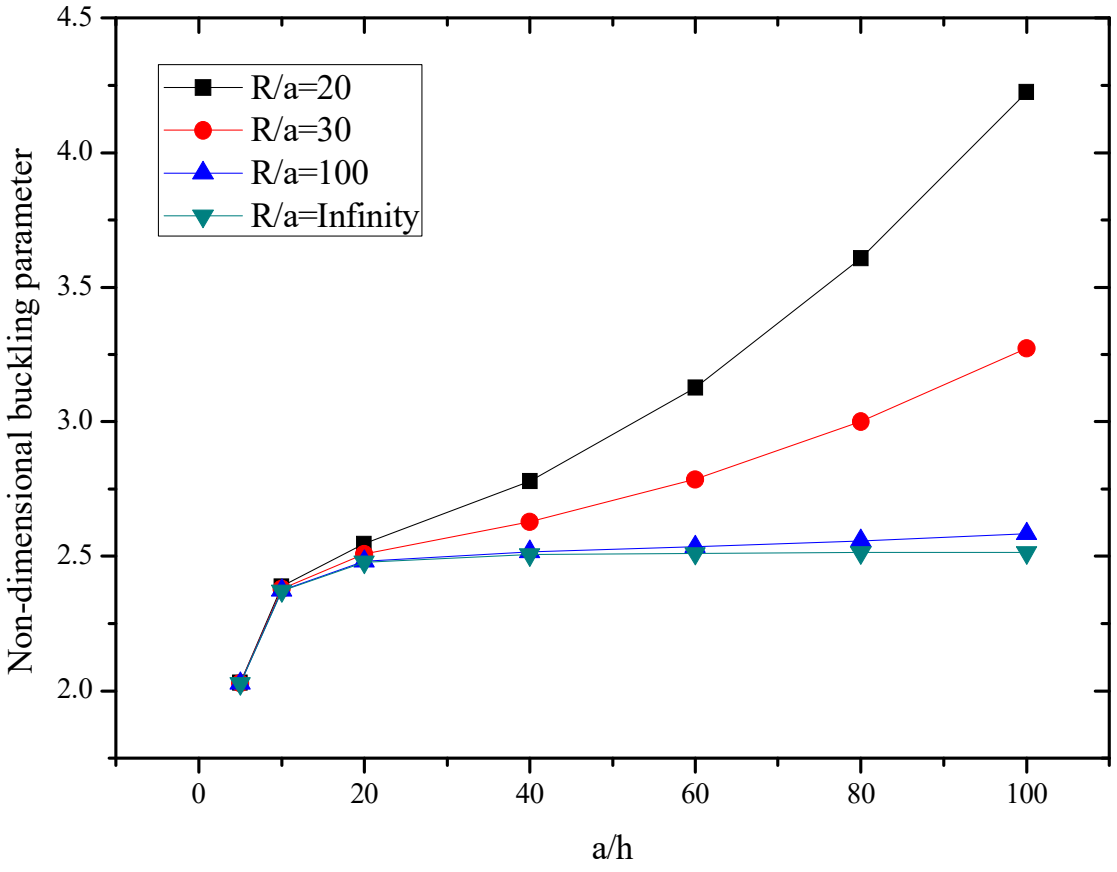

Figure 4.2 Non-dimensional buckling parameter of spherical shell (Al/ZrO_2) and plate (*R/a*=∞) under biaxial load with varying *a/h* ratio and *R/a* (*N*=3)

4.3 Finite Element Method

In this section, the results of buckling response are obtained by FEM using IHSDT for functionally graded shells and compared with the analytical methodology to validate the formulation for simply supported boundary conditions. The different parameters as span-thickness, power index and curvature ratio are discussed for the buckling response.

Boundary conditions for the FGM shells model is discussed as:

a. Simply supported boundary condition (S):

$$u_0 = w_0 = \phi_x = \theta_x = 0 \text{ at } x = 0, a$$
$$v_0 = w_0 = \phi_y = \theta_y = 0 \text{ at } y = 0, b \quad (4.2)$$

b. Clamped boundary condition (C):

$$u_0 = v_0 = w_0 = \phi_x = \phi_y = \theta_x = \theta_y = 0 \quad (4.3)$$

4.3.1 Convergence and Validation of Results Obtained using FEM

In order to ensure the convergence of present FE analysis, an FGM shell composed of Al/Al_2O_3 is considered. Figure 4.5 shows the NDBP obtained for different boundary conditions applied

on FGM shells. The three conditions are SSSS (Simply supported boundary conditions), CCCC (Clamped boundary conditions) and SCSC (two clamped and two simply supported boundary conditions). The FGM spherical shell whose material properties vary according to power law with N=1 under uniaxial load for a/h=20, R/a=10 is studied and from the figure it is observed that after 8 number of elements, the value of non-dimensional buckling parameter converges.

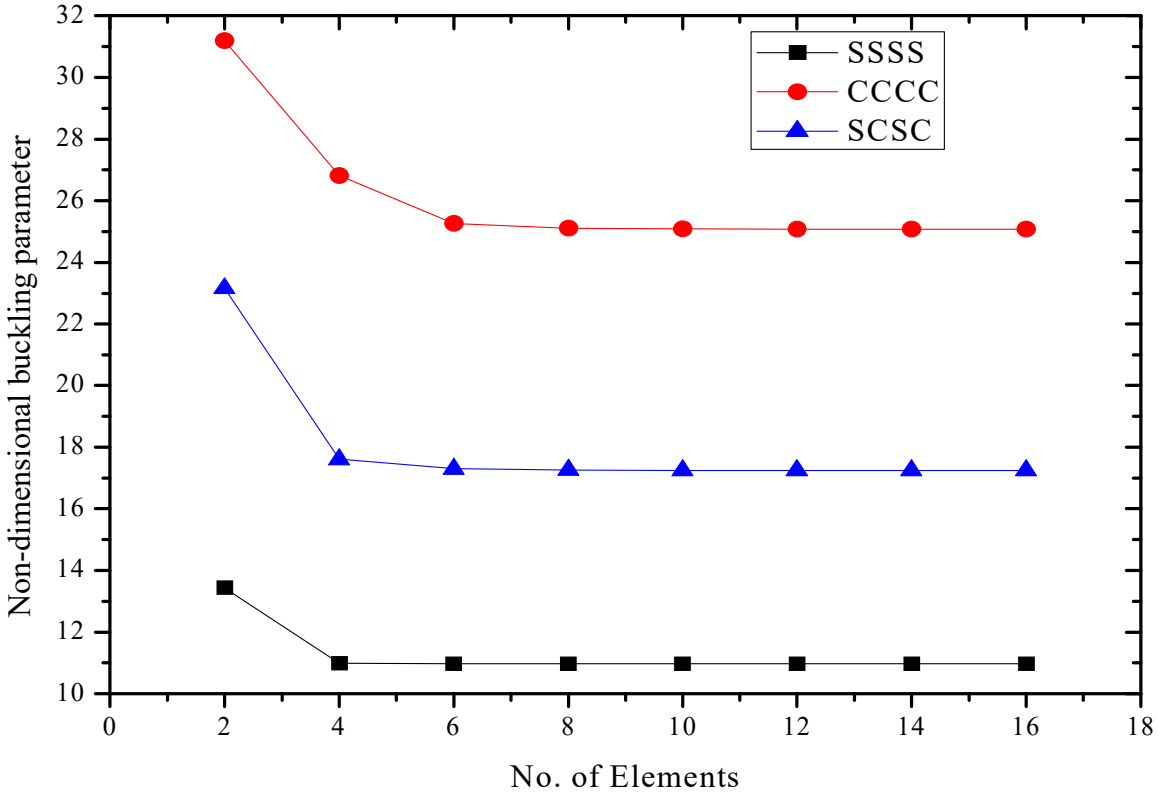

Figure 4.3 Effect of number of elements on the rate of convergence of FGMs Spherical Shells (N=1, a/h=20, R/a=10)

Table 4.2 illustrates the value of NDBP for different values of span-thickness ratio, power index and curvature ratio under simply supported boundary condition obtained by using both analytical and finite element method. It is observed that the results are in close agreement with closed form solution. Furthermore, to see the closeness graphically between the results of close form solution and finite element method, the case of spherical shell under biaxial load with varying a/h ratio and R/a = 50 demonstrates in Figure 4.3.

Table 4.2 Validation of FEM using Analytical results of non-dimensional buckling parameter of cylindrical shells (Al/Al_2O_3) under uniaxial load and simply supported condition

a/h	*N*	*R/a*=10		*R/a* =50	
		CFS	FEM	CFS	FEM
5	3	5.6640	5.6576	5.6511	5.6448
10		6.6220	6.6205	6.5708	6.5693
20		7.0622	7.0621	6.8572	6.8571
40		7.7766	7.7770	6.9567	6.9571
100		12.2810	11.0683	7.1570	7.1579
5	5	5.0569	5.0542	5.0463	5.0436
10		6.0756	6.0751	6.0333	6.0329
20		6.5198	6.5199	6.3507	6.3509
40		7.1318	7.1318	6.4551	6.4555
100		10.8533	10.2577	6.6268	6.6275
5	7	4.7650	4.7614	4.7555	4.7519
10		5.7929	5.7921	5.7551	5.7544
20		6.2322	6.2323	6.0811	6.0812
40		6.7906	6.7910	6.1862	6.1865
100		10.1208	9.8234	6.3430	6.3436
5	9	4.5794	4.5733	4.5706	4.5645
10		5.5835	5.5819	5.5484	5.5468
20		6.0086	6.0086	5.8683	5.8681
40		6.5319	6.5323	6.0934	5.9708
100		9.6262	9.4770	6.1175	6.1182

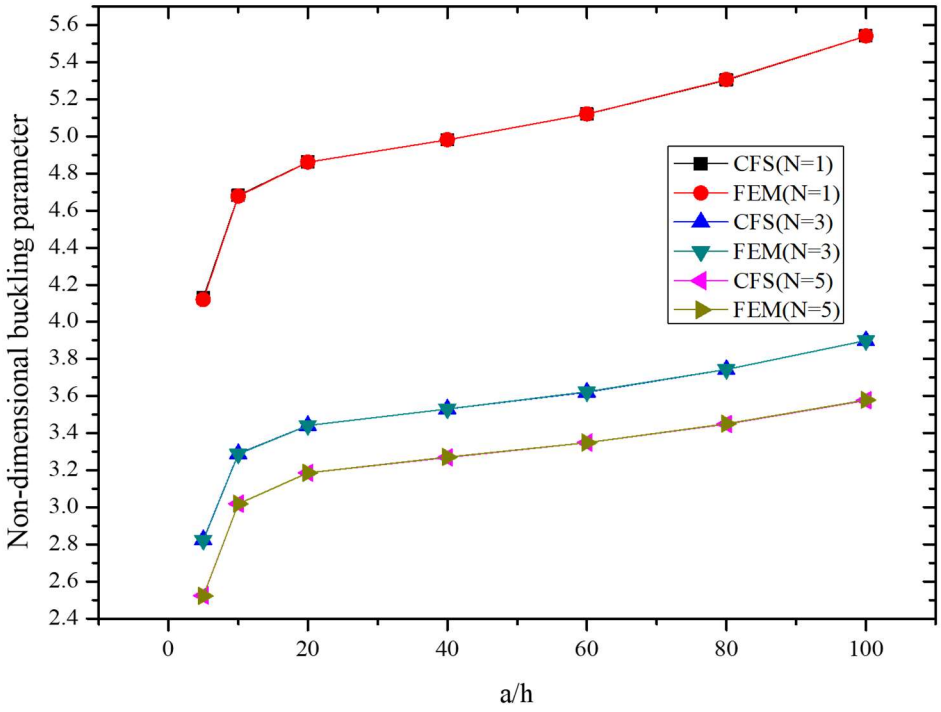

Figure 4.3 Validation of FEM using analytical response of spherical shell under biaxial load with varying *a/h* ratio (*R/a*=50, *N*=5)

Table 4.3 shows the validation of the finite element method using closed form solutions for the non-dimensional buckling response of the FGM cylindrical shells (Al/Al_2O_3) under arbitrary loads where the span-thickness ratio and curvature ratio remains constant. It is observed that as the arbitrary load varies the non-dimensional buckling load decreases independent of the value of the power index.

Table 4.3 Non-dimensional buckling parameter of FG cylindrical shells (Al/Al_2O_3) under arbitrary loads (*a/h*=40, *R/a*=30)

K	*N*=2		*N* =5		*N* =7	
	CFS	FEM	CFS	FEM	CFS	FEM
-0.4	12.8681	12.8685	10.842	10.8426	10.3849	10.3854
-0.2	9.6511	9.6514	8.1315	8.132	7.7887	7.7891
0	7.7208	7.7211	6.5052	6.5056	6.2309	6.2313
0.2	6.434	6.4343	5.421	5.4213	5.1924	5.1927
0.4	5.5149	5.5151	4.6466	4.6468	4.4507	4.4509
0.6	4.8255	4.8257	4.0658	4.066	3.8943	3.8945
0.8	4.2894	4.2895	3.614	3.6142	3.4616	3.4618
1	3.8604	3.8606	3.2526	3.2528	3.1155	3.1156

4.3.2 Buckling Analysis of FGM Cylindrical Shells

The FGM singly curved or cylindrical shells are studied for two different combinations of metal/ceramic i.e. Aluminum/Alumina (Al/Al_2O_3) and Aluminum/Zirconia (Al/ZrO_2) subjected to in-plane loads under different boundary conditions. Non-dimensional buckling parameter under CCCC and SCSC boundary conditions are discussed in this section. Table 4.4 lists the results for FGM cylindrical shell composed of Aluminum/Alumina under uniaxial load with varying values of span-thickness ratio, power index and curvature ratio when all the edges are clamped. It is observed that for constant value of power index and curvature ratio, the non-dimensional buckling load increases as the span-thickness ratio increases.

Table 4.4 Non-dimensional buckling parameter of cylindrical shells (Al/Al_2O_3) under uniaxial load and all clamped boundary condition

a/h	*N*	*R/a*=5	*R/a* =10	*R/a* =50	*R/a* =100
5	1	14.4074	14.3590	14.3431	14.3426
10		21.4488	21.0780	20.9558	20.9520
20		25.7975	24.1926	23.6411	23.6235
40		28.8080	26.7105	24.5326	24.4604
100		33.1677	30.1184	25.4957	25.0458
5	2	10.9117	10.8765	10.8650	10.8646
10		16.5461	16.2646	16.1718	16.1688
20		20.0435	18.8113	18.3877	18.3742
40		22.4441	20.8028	19.1254	19.0698
100		25.8311	23.4803	19.8834	19.5368
5	4	8.3778	8.3734	8.3720	8.3720
10		13.7428	13.5404	13.4736	13.4715
20		17.0465	16.1134	15.7944	15.7842
40		19.3699	17.8557	16.5733	16.5311
100		22.0765	20.2755	17.2199	16.9556
5	8	6.9488	6.9454	6.9444	6.9443
10		12.0935	11.9414	11.8912	11.8896
20		15.2850	14.5489	14.2988	14.2909
40		17.5997	16.1343	15.1154	15.0821
100		19.8570	18.4237	15.6913	15.4819

For the constant value of span-thickness ratio and curvature ratio, NDBP decreases as the value of power index increases. The NDBP of FGM cylindrical shells composed of Aluminum/Zirconia subjected to biaxial load is obtained taking constant value of span-thickness ratio as 20 with varying power index and curvature ratio. It is noted that as the curvature ratio increases, the results of non-dimensional buckling load decrease as shown in Figure 4.4.

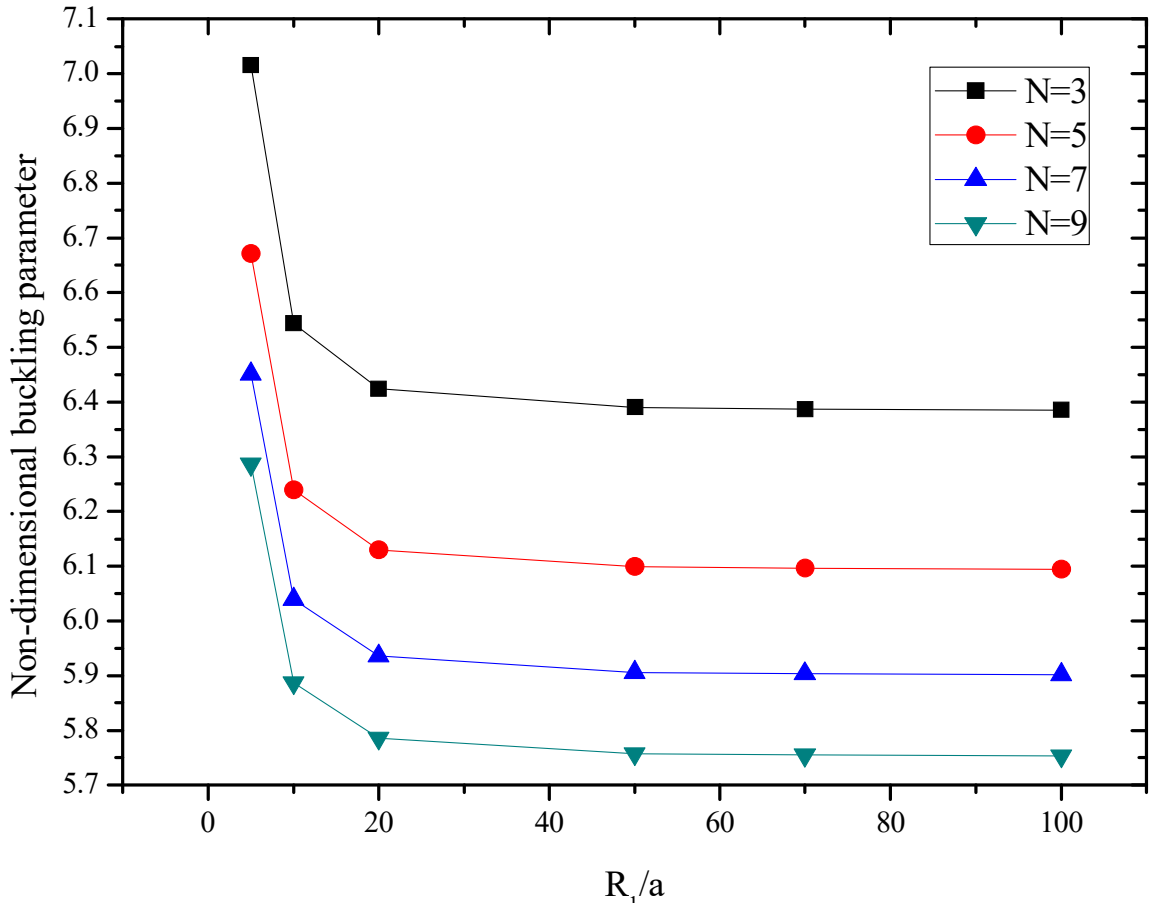

Figure 4.4 Non-dimensional buckling parameter of cylindrical shells (Al/ZrO_2) under biaxial load and all clamped condition with varying *R/a* (*a/h*=20)

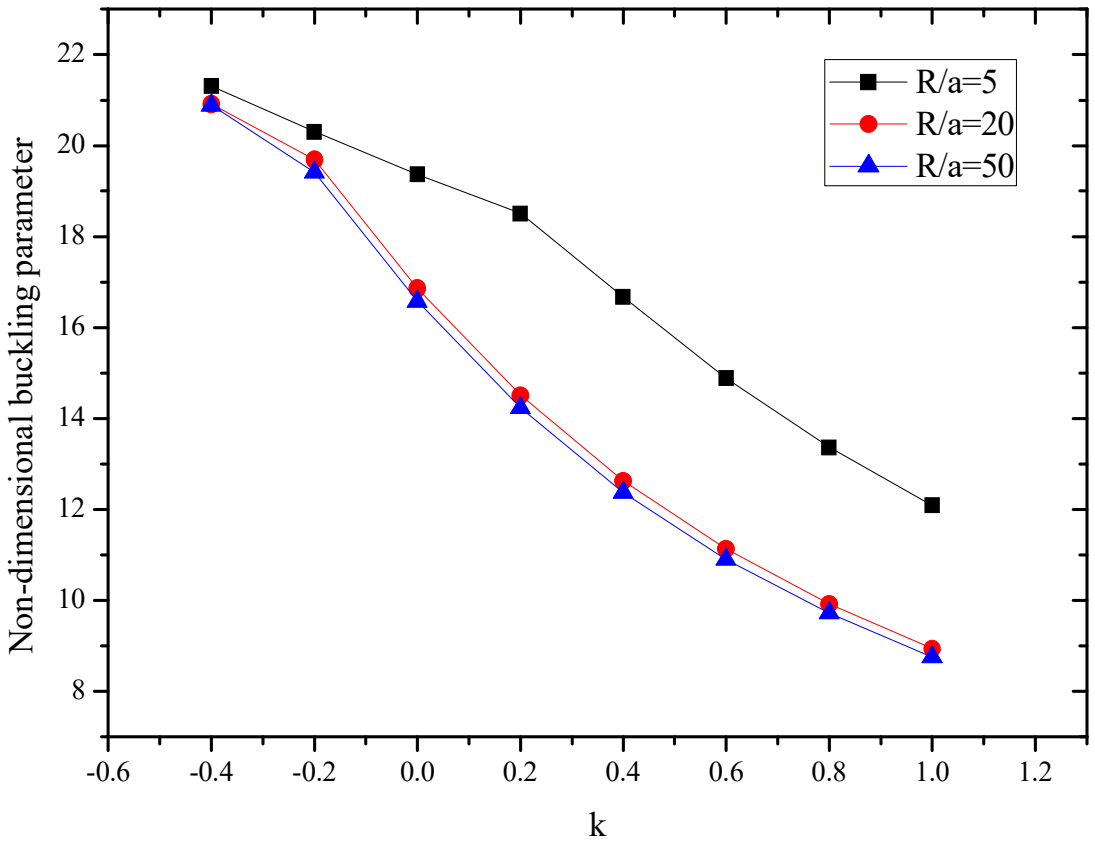

Figure 4.5 Non-dimensional buckling parameter of cylindrical shells (Al/Al_2O_3) under arbitrary loads and clamped boundary condition (*a/h*=40, *N*=4)

Figure 4.5 illustrates that the non-dimensionality of the buckling parameter for cylindrical shells (Al/Al_2O_3) which is under arbitrary loads for constant value of span-thickness ratio and power index, it is observed that independent of the curvature ratio, non-dimensional buckling response decreases as the load increases. Table 4.5 lists the non-dimensional buckling parameter for the cylindrical shells composed of Al/ZrO_2 under arbitrary loads for SCSC boundary conditions with the constant value of span-thickness ratio and curvature ratio. NDBP decreases with as the arbitrary load varies for a constant value of a load and shows same observations for the variation in the power index as the load is constant. Figure 4.6 illustrates the non-dimensional buckling results increases for the variation in the span-thickness ratio under uniaxial load for SCSC boundary condition but the large value for non-dimensional buckling obtained for the shallow cylindrical shells.

Table 4.5 Non-dimensional buckling of cylindrical shells (Al/ZrO_2) under arbitrary loads and SCSC boundary condition (*a/h*=20, *R/a*=100)

K	*N*=1	*N*=3	*N*=5	*N*=7
-0.4	13.1507	11.3479	10.8331	10.4911
-0.2	11.0851	9.5719	9.1405	8.8525
0	9.4919	8.198	7.8294	7.5829
0.2	8.2636	7.1376	6.8169	6.6023
0.4	7.3011	6.3061	6.0227	5.8331
0.6	6.5316	5.6413	5.3876	5.218
0.8	5.9047	5.0996	4.8702	4.7168
1	5.3852	4.6507	4.4414	4.3015

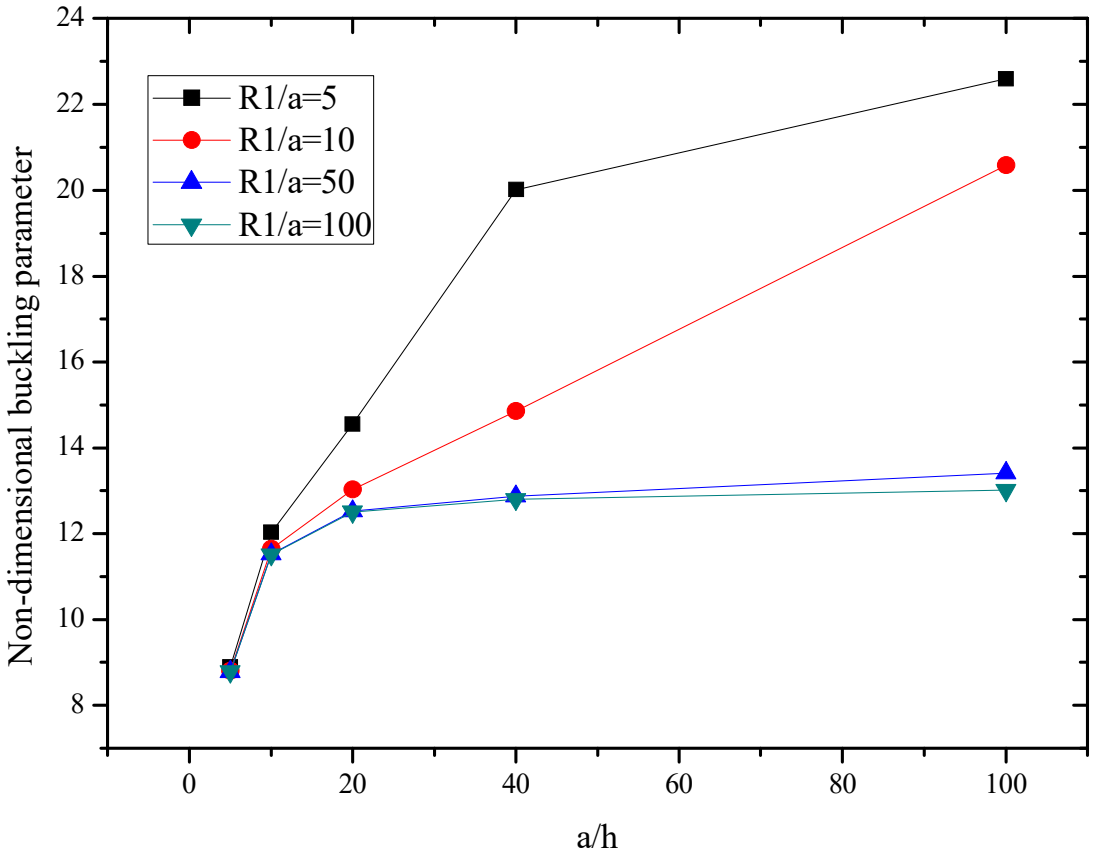

Figure 4.6 Non-dimensional buckling parameter of cylindrical shells (Al/Al_2O_3) under uniaxial load and SCSC with varying *a/h* and *R/a* ratio (*N*=2)

4.3.3 Buckling Analysis of FGM Spherical Shells

In this section, the FGM spherical shells are being discussed for the different material properties i.e. Aluminium/Alumina and Aluminium/Zirconia for different values of power index, curvature ratio and span-thickness ratio. Table 4.6 illustrates the results of NDBP increases for a constant value of span-thickness ratio and curvature ratio irrespective of the value of power index under SCSC boundary condition.

Table 4.6 Non-dimensional buckling parameter of spherical shells (Al/Al_2O_3) under biaxial load with condition SCSC

a/h	*N*	*R/a*=5	*R/a*=10	*R/a*=50	*R/a*=100
5	1	6.7321	6.5877	6.5414	6.5399
10		9.1699	8.6119	8.4326	8.427
20		12.0315	9.8481	9.1409	9.1187
40		18.5929	12.2202	9.4237	9.3354
100		39.3003	21.1717	10.1079	9.5582
5	2	5.1436	5.0322	4.9964	4.9953
10		7.099	6.6688	6.5305	6.5262
20		9.3451	7.6625	7.1174	7.1004
40		14.4579	9.5031	7.3483	7.2803
100		30.5305	16.4533	7.8793	7.4558
5	4	4.1234	4.0381	4.0107	4.0099
10		5.9526	5.6237	5.518	5.5147
20		7.8399	6.5551	6.1394	6.1264
40		12.1976	8.0139	6.3702	6.3184
100		24.8977	13.7562	6.7912	6.4685
5	8	3.5314	3.4636	3.4418	3.4411
10		5.2739	5.0128	4.9289	4.9263
20		6.9265	5.9073	5.5779	5.5676
40		10.8339	7.1138	5.8112	5.7702
100		20.9945	12.1027	6.1598	5.9043

Figure 4.6 shows that NDBP increases as the spherical shell goes from thin to thick shells irrespective of the value of the power index as the curvature ratio remains constant under uniaxial and all clamped boundary conditions. Table 4.7 lists the non-dimensional buckling

load of FGM spherical shells increase under all clamped and SCSC boundary conditions where parameters such as span-thickness ratio and curvature ratio remain the same. It is observed that the buckling load reduces as the value of *k* increases.

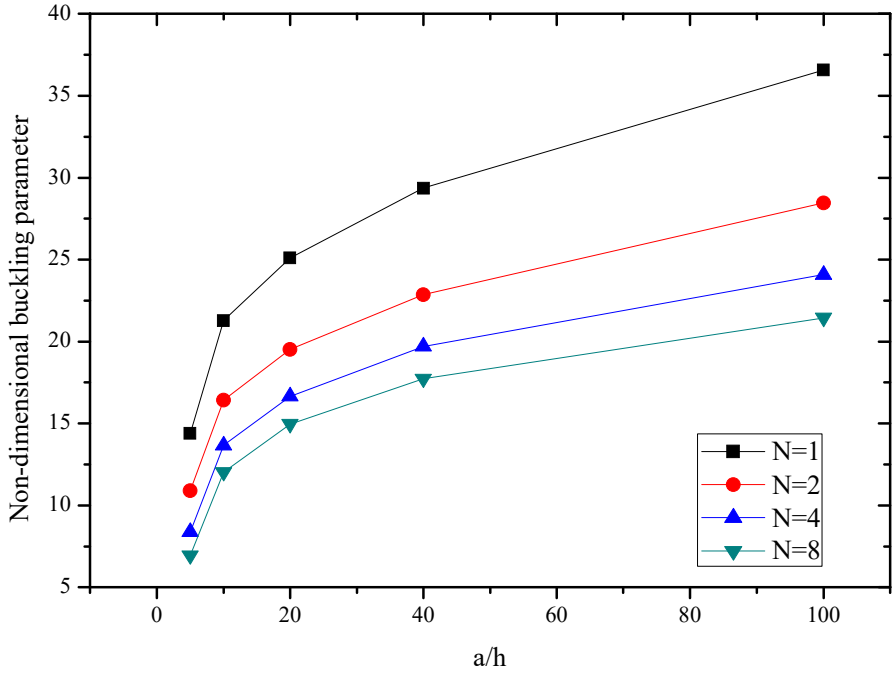

Figure 4.7 Non-dimensional buckling parameter of spherical shells (Al/Al_2O_3) under uniaxial load and all clamped condition with varying *a/h* ratio (*R/a*=10)

Table 4.7 Non-dimensional buckling load of FGM spherical shells (Al/Al_2O_3) under arbitrary loads for *a/h*=60, *R/a*=75 for power index (*N*=1,4) under all clamped and SCSC boundary conditions

K	*N*=1		*N*=4	
	CCCC	SCSC	CCCC	SCSC
-0.4	31.4785	23.1558	21.2805	15.6776
-0.2	29.2173	19.4652	19.7561	13.1791
0	24.8987	16.6549	16.8406	11.2762
0.2	21.3662	14.5001	14.4533	9.817
0.4	18.5705	12.815	12.5629	8.6758
0.6	16.3548	11.4689	11.0644	7.7643
0.8	14.5767	10.3723	9.8615	7.0217
1	13.1277	9.4635	8.8813	6.4063

CHAPTER 5 BUCKLING ANALYSIS OF FGM SHELLS USING EXPONENTIAL LAW

5.1 Introduction

In this chapter, FGM shells modelled using exponential law are discussed for the buckling response using the mentioned methodology in the previous chapters. Analysis of buckling parameter is carried out by programming the generalized MATLAB code for closed form solution as well as finite element method and further the responses of the non-dimensional buckling parameter is obtained by using given expression:

$$\widetilde{N}_{cr} = \frac{\lambda a^2}{E_m h^3} \tag{5.1}$$

The following material properties are used for FGMs Shells [Kulkarni *et al.* (2013)]:

Aluminum/Alumina (Al/Al_2O_3): E_m=70GPa; E_c=380GPa; ν = 0.3

Aluminum/Zirconia (Al/ZrO_2): E_m=70GPa; E_c=168GPa; ν = 0.3

5.2 Analytical Method

FGM spherical shells are considered under in-plane loads with simply supported boundary conditions by using closed form solution to obtain results for buckling response. Table 5.1 shows the non-dimensional buckling parameter results for the spherical shells composed of Al/Al_2O_3 under uniaxial in-plane loads where the effect of span-thickness ratio, power index and curvature ratio are observed. With the increase of span-thickness ratio and constant power index and curvature ratio, the non-dimensional buckling parameter increases. And for the constant power index and span-thickness ratio, the non-dimensional buckling load decreases with the increasing curvature ratio (*R/a*).

The FGM spherical shells whose material properties gradation are according to the exponential law and composed of Al/ZrO_2 under biaxial load with constant value of power index and varying value of curvature ratio from shallow to deep spherical shells and span-thickness ratio from thin to thick spherical shells, shows the non-dimensional buckling parameter increases for deep shells and no much variation for the shallow shells as shown in Figure 5.1.

Table 5.1 Non-dimensional buckling parameter of spherical shell (Al/Al_2O_3) under uniaxial load

a/h	*N*	*R/a*=10		*R/a*=50	
		Analytical	FEM	Analytical	FEM
5	3	5.664	5.6576	5.6511	5.6448
10		6.622	6.6205	6.5708	6.5693
20		7.0622	7.0621	6.8572	6.8571
40		7.7766	7.777	6.9567	6.9571
100		12.281	11.0683	7.157	7.1579
5	5	5.0569	5.0542	5.0463	5.0436
10		6.0756	6.0751	6.0333	6.0329
20		6.5198	6.5199	6.3507	6.3509
40		7.1318	7.1318	6.4551	6.4555
100		10.8533	10.2577	6.6268	6.6275
5	7	4.765	4.7614	4.7555	4.7519
10		5.7929	5.7921	5.7551	5.7544
20		6.2322	6.2323	6.0811	6.0812
40		6.7906	6.791	6.1862	6.1865
100		10.1208	9.8234	6.343	6.3436
5	9	4.5794	4.5733	4.5706	4.5645
10		5.5835	5.5819	5.5484	5.5468
20		6.0086	6.0086	5.8683	5.8681
40		6.5319	6.5323	6.0934	5.9708
100		9.6262	9.477	6.1175	6.1182

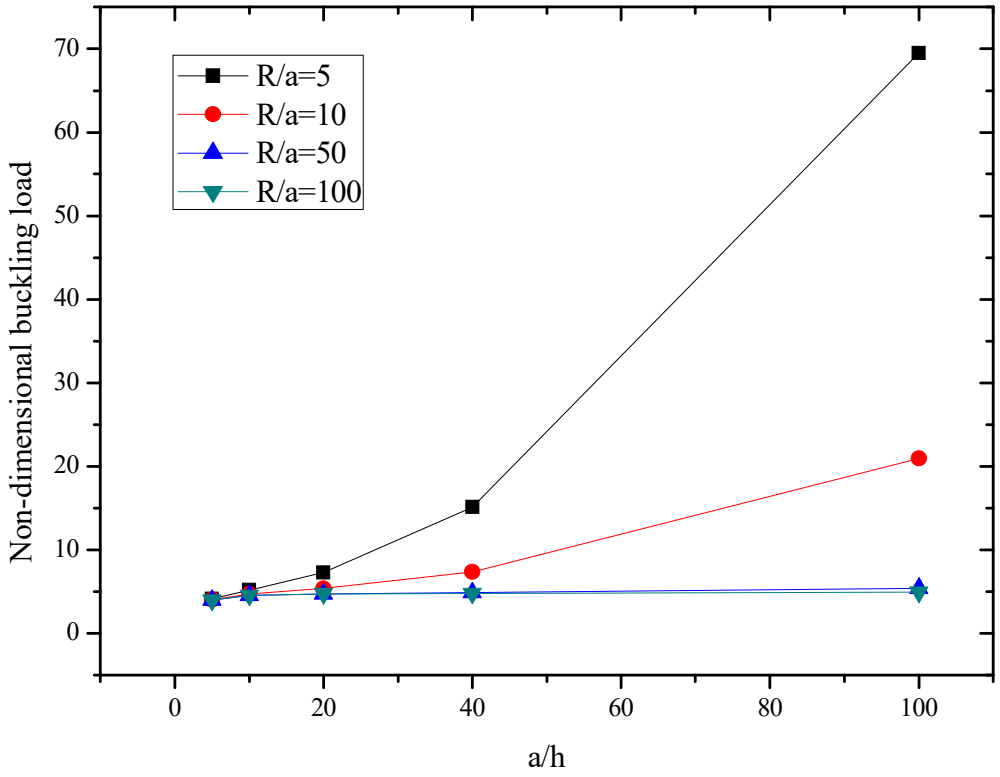

Figure 5.1 Non-dimensional buckling parameter of spherical shell (Al/ZrO_2) under biaxial load with varying *a/h* ratio and *R/a* (*N*=2)

5.3 Finite Element Method

Finite element method is implemented to obtain the results for non-dimensional buckling parameter by using inverse hyperbolic shear deformation theory for functionally graded doubly curved spherical and cylindrical shells and compared with analytical to validate the formulation by discussing the different parameters as span-thickness ratio, curvature ratio and power index taking different boundary conditions under uniaxial and biaxial in-plane loads.

Boundary conditions for the FGM shells model is discussed as:

c. Simply supported boundary condition (S):

$$u_0 = w_0 = \phi_x = \theta_x = 0 \text{ at } x = 0, a$$
$$v_0 = w_0 = \phi_y = \theta_y = 0 \text{ at } y = 0, b \quad (5.2)$$

d. Clamped boundary condition (C):

$$u_0 = v_0 = w_0 = \phi_x = \phi_y = \theta_x = \theta_y = 0 \quad (5.3)$$

5.2.1 Convergence and Validation of Results Obtained using FEM

Finite element method is implemented on the FGM shells and to validate the FEM, the result of closed form solutions is compared with the results of FEM. Table 5.2 illustrates the validation of the generalized FEM MATLAB code taking a numerical example of functionally

graded cylindrical shells composed of Aluminium/Zirconia under uniaxial in-plane load taking simply supported boundary conditions. It is found that finite element method shows the closeness with the closed form solution.

Figure 5.1 demonstrates the convergence of the finite element method for the non-dimensional buckling parameter for different boundary conditions. It is observed that after eight number of elements the results obtained are close to each other. Hence, for further studies, a mesh size of 8x8 is considered.

Table 5.2 Validating the closed form and finite element solution for non-dimensional buckling parameter of cylindrical shells (Al/ZrO_2) under SSSS boundary condition and uniaxial in-plane load

a/h	*N*	*R/a*=10		*R/a*=50	
		Analytical	FEM	Analytical	FEM
5	3	5.664	5.6576	5.6511	5.6448
10		6.622	6.6205	6.5708	6.5693
20		7.0622	7.0621	6.8572	6.8571
40		7.7766	7.777	6.9567	6.9571
100		12.281	11.0683	7.157	7.1579
5	5	5.0569	5.0542	5.0463	5.0436
10		6.0756	6.0751	6.0333	6.0329
20		6.5198	6.5199	6.3507	6.3509
40		7.1318	7.1318	6.4551	6.4555
100		10.8533	10.2577	6.6268	6.6275
5	7	4.765	4.7614	4.7555	4.7519
10		5.7929	5.7921	5.7551	5.7544
20		6.2322	6.2323	6.0811	6.0812
40		6.7906	6.791	6.1862	6.1865
100		10.1208	9.8234	6.343	6.3436
5	9	4.5794	4.5733	4.5706	4.5645
10		5.5835	5.5819	5.5484	5.5468
20		6.0086	6.0086	5.8683	5.8681
40		6.5319	6.5323	6.0934	5.9708
100		9.6262	9.477	6.1175	6.1182

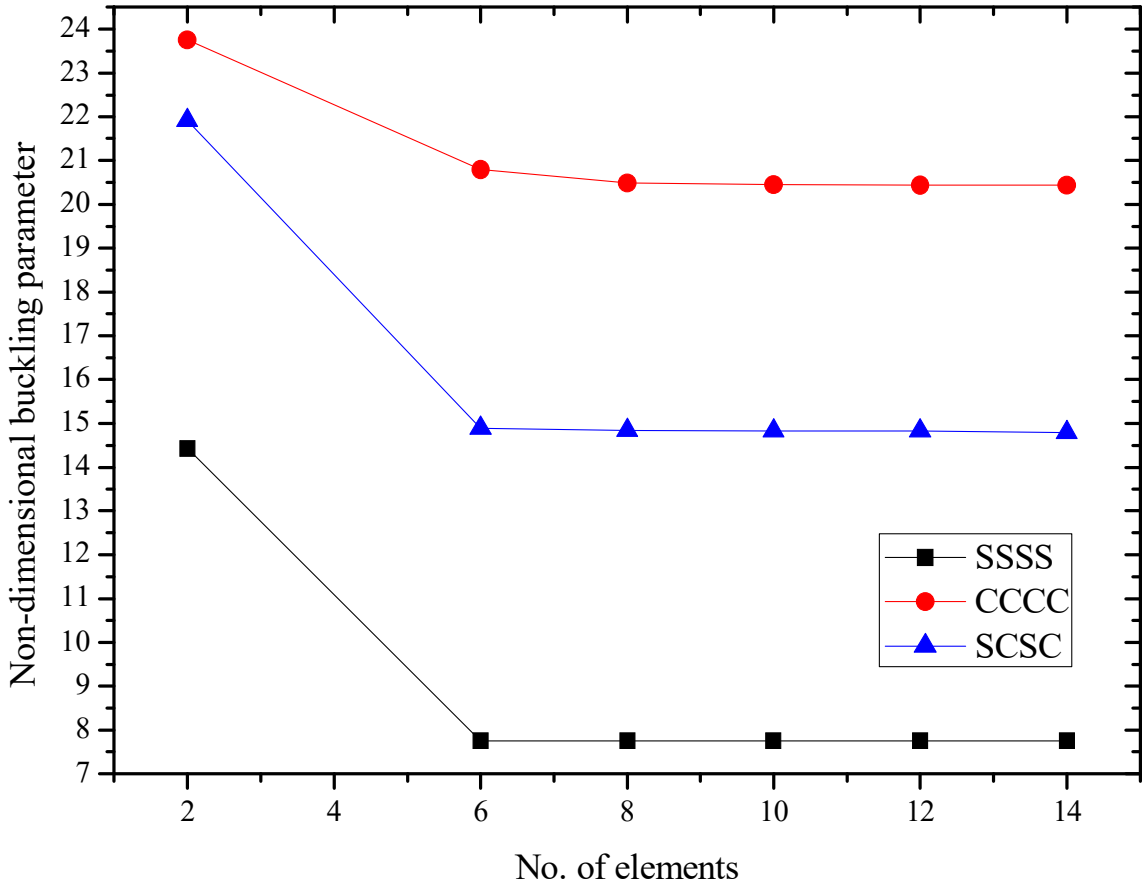

Figure 5.2 Convergence of non-dimensional buckling parameter for FGM cylindrical shells (Al/ZrO_2) under biaxial (*N*=3, *a/h*=40, *R/a*=50)

5.2.2 Buckling Analysis of Cylindrical Shells

Functionally graded cylindrical shells are studied using finite element method for the effects of different parameter on the non-dimensionality of buckling response under different loading and boundary conditions. Table 5.3 lists the NDBP results for the cylindrical shells which consist of properties of Aluminium/Alumina under biaxial load where all clamped and SCSC boundary conditions are considered. It is observed that the non-dimensional buckling load decreases for constant value of span-thickness ratio and power index under biaxial load for both boundary conditions i.e. CCCC and SCSC for varying curvature ratio. Figure 5.3 shows that under any boundary condition the results of NDBP increases for cylindrical shells having constant value of power index and increasing value of span-thickness ratio independent of the value of curvature ratio.

Table 5.3 Non-dimensional buckling load of cylindrical shells (Al/Al_2O_3) under biaxial load with CCCC and SCSC boundary conditions

a/h	*N*	*R/a*=5		*R/a*=20		*R/a*=100	
		CCCC	SCSC	CCCC	SCSC	CCCC	SCSC
5	1	4.937	3.8494	4.8884	3.7921	4.8853	3.7884
10		6.9727	5.2513	6.7813	5.033	6.769	5.0189
20		8.3426	6.3932	7.5904	5.5425	7.5415	5.4874
40		10.8515	9.1104	7.9795	5.8472	7.7851	5.6284
100		15.9516	14.4055	9.1473	7.0677	7.9554	5.7218
5	2	8.2643	6.4208	8.1742	6.3148	8.1684	6.308
10		11.4541	8.6272	11.0988	8.2223	11.0759	8.1963
20		13.7219	10.5773	12.3268	8.9995	12.236	8.8972
40		18.2505	15.5294	12.9641	9.5153	12.6028	9.1089
100		26.3005	23.6849	15.101	11.7631	12.8928	9.2675
5	4	24.2714	18.6617	23.8952	18.225	23.8711	18.1969
10		31.8938	24.0968	30.4111	22.4128	30.3125	22.3043
20		38.858	30.7038	33.0685	24.1494	32.6882	23.7211
40		56.0977	49.9956	34.9824	25.8688	33.4711	24.1678
100		75.4624	67.2102	43.5646	35.0401	34.4492	24.7037

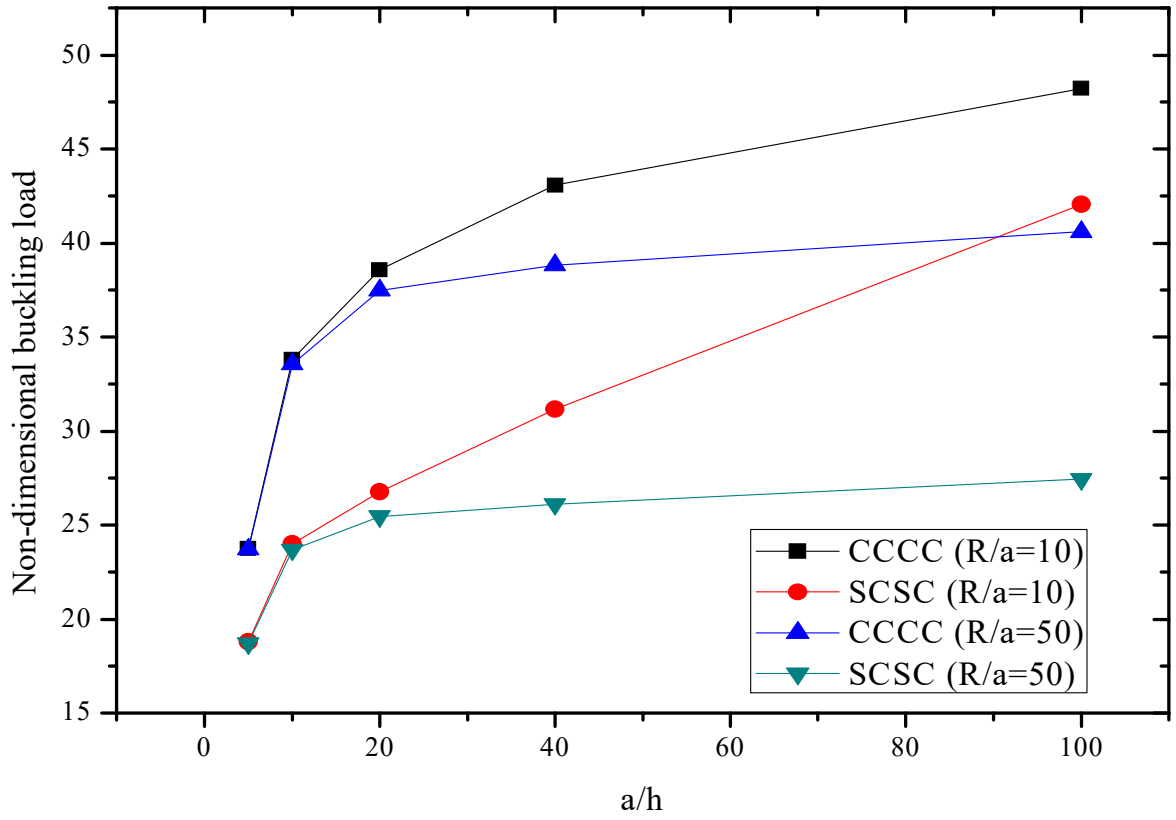

Figure 5.3 Non-dimensional buckling load of cylindrical shells (Al/ZrO_2) under uniaxial load for *N*=3

5.2.3 Buckling Analysis of Spherical Shells

In this section, FGM doubly curved spherical shells are considered consisting of different material properties under different boundary conditions. Table 5.4 illustrates that NDBP results increase for the spherical shells of Aluminium/Zirconia under uniaxial in-plane load for CCCC and SCSC boundary conditions as the span-thickness ratio increases for the constant value of curvature ratio and power index. Figure 5.4 demonstrates the results of NDBP increases with the increase in the value of span-thickness ratio irrespective of the power index for curvature ratio equals to 50. Moreover, a clamped shell possesses higher buckling load relative to shell with SCSC condition. It is also noted that the shell with higher value of power index (*N*) possess higher buckling load. This is due to increment in overall stiffness of the shell due to increased *N*.

Table 5.4 Non-dimensional buckling load of doubly curved spherical shells (Al/ZrO_2) under uniaxial load for different boundary conditions

a/h	*N*	*R/a*=10		*R/a*=40		*R/a*=100	
		CCCC	SCSC	CCCC	SCSC	CCCC	SCSC
5	1	8.1649	6.6919	8.1417	6.6594	8.1404	6.6575
10		12.5653	9.0155	12.3971	8.8671	12.3875	8.8588
20		14.9824	10.3111	14.2367	9.709	14.1937	9.6749
40		17.6161	12.4118	14.9536	10.0615	14.7775	9.9249
100		21.5565	19.2266	16.3111	10.981	15.2381	10.1375
5	3	23.8352	18.8424	23.7306	18.7156	23.7247	18.7085
10		34.2495	24.2759	33.6053	23.7235	33.5686	23.6924
20		40.3863	27.793	37.636	25.5697	37.4756	25.4434
40		46.969	35.0516	39.4214	26.5052	38.7701	25.9997
100		60.9253	54.3372	44.1058	29.7799	40.1999	26.6783

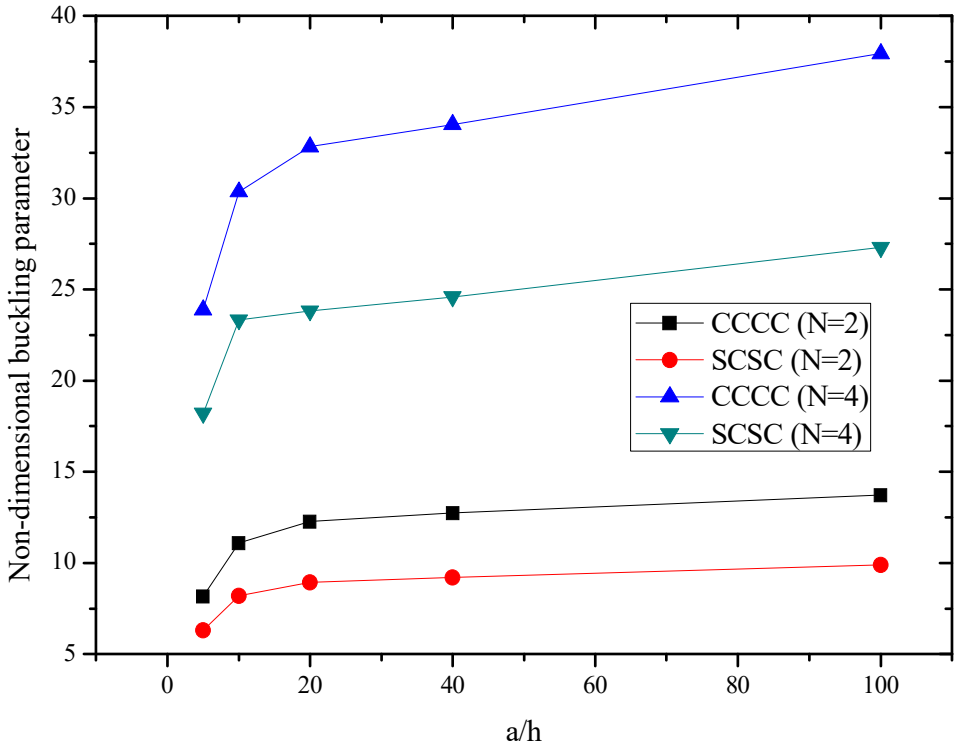

Figure 5.4 Non-dimensional buckling parameter of doubly curved spherical shells (Al/Al_2O_3) under biaxial load for *R/a*=50 under different boundary conditions

CHAPTER 6 CONCLUSION AND FUTURE SCOPE

6.1 Concluding Remarks

The inverse hyperbolic shear deformation theory is implemented for the buckling response of functionally graded cylindrical and spherical shells. The theory is based on the shear strain function which satisfies the traction free boundary conditions and also satisfies the criteria of continuity and differentiability. The governing differential equations are obtained using principle of virtual work and solved via Navier type exact solution methodology. Analysis of buckling load is done by using closed form solutions as well as finite element method. The results for the analytical are validated by comparing the special case i.e. FGM plates with the existing theories. On the basis of the present work, the following conclusions can be made:

I. FGM cylindrical and spherical shells are modelled using inverse hyperbolic shear deformation theory. The material gradation properties of the functionally graded materials vary according to the power and exponential law.

II. Analytical results of the buckling response for FGM spherical shells generated using generalized MATLAB code is validated by taking curvature ratio equals to infinite that makes the FGM spherical shells to FGM plates and compared with the existing theories.

III. The effect of span-thickness ratio, power index and curvature ratio studied for non-dimensional buckling parameter for both material gradation properties law i.e. power law and exponential law.

IV. Functionally graded doubly curved spherical and cylindrical shells shows similar trends for the material gradation properties according to the power law. The non-dimensional buckling parameter increases as the span-thickness ratio varies with the constant value of power index and curvature ratio.

V. For constant value of span-thickness ratio and curvature ratio, the non-dimensional buckling parameter increases with the increase in the power index same trend of the non-dimensional buckling is observed for varying value of curvature ratio under in-plane load and boundary conditions (SSSS, CCCC and SCSC).

VI. As the material properties of FGM spherical and cylindrical shells modelled according to the exponential law shows the same trend of the buckling response for both case of shells. The NDBP increases with the variation in the power index for constant value of span-thickness and curvature ratio as well as with the variation in the span-thickness ratio.

VII. For the constant value of span-thickness ratio and power index, the non-dimensional buckling parameter decreases with the increase in the curvature ratio for spherical as well as cylindrical shells for exponential law.

Publications from the Present Work

- Rajpoot R.R., Neeraj H., Grover N., Khanna K., Deformation characteristics of functionally graded plates using a non-polynomial shear deformation theory, 1st Symposium and Workshop for Analytical Youth on Applied Mechanics (SWAYAM 2018), BITS Pilani, K. K. Birla Goa Campus, Goa. pp. 33-34
- Rajpoot R.R., Grover N., Khanna K., Analytical investigation for buckling characteristics of FG doubly curved spherical and cylindrical shells, under preparation.
- Rajpoot R.R., Grover N., Khanna K., Finite element framework of inverse hyperbolic shear deformation theory for buckling response of FG shells, under preparation.

6.2 Scope for Future Work

- Study of the functionally graded doubly curved spherical and cylindrical shells for the non-linear problems.
- Study of FGM shells under thermal load using IHSDT for arbitrary geometry of the shells.

References

Aydogdu M. "A new shear deformation theory for laminated composite plates." *Composite structures* 89.1 (2009): 94-101.

Bagherizadeh E., Kiani Y. and Eslami M.R. "Mechanical buckling of functionally graded material cylindrical shells surrounded by Pasternak elastic foundation." *Composite Structures* 93.11 (2011): 3063-3071.

Belabed Z., Houari M.S.A., Tounsi A., Mahmoud S.R. and Bég O.A. "An efficient and simple higher order shear and normal deformation theory for functionally graded material (FGM) plates." *Composites Part B: Engineering* 60 (2014): 274-283.

Carrera E. "Theories and finite elements for multilayered, anisotropic, composite plates and shells." *Archives of Computational Methods in Engineering* 9.2 (2002): 87-140.

Chi S.H. and Chung Y.L. "Mechanical behavior of functionally graded material plates under transverse load-Part I: Analysis." *International Journal of Solids and Structures* 43.13 (2006): 3657-3674.

Chi S.H. and Chung Y.L. "Mechanical behavior of functionally graded material plates under transverse load-Part II: Numerical results." *International Journal of Solids and Structures* 43.13 (2006): 3675-3691.

El Meiche N., Tounsi A., Ziane N. and Mechab I. "A new hyperbolic shear deformation theory for buckling and vibration of functionally graded sandwich plate." *International Journal of Mechanical Sciences* 53.4 (2011): 237-247.

Feldman E. and Aboudi J. "Buckling analysis of functionally graded plates subjected to uniaxial loading." *Composite Structures* 38.1-4 (1997): 29-36.

Grover N., Maiti D.K. and Singh B.N. "A new inverse hyperbolic shear deformation theory for static and buckling analysis of laminated composite and sandwich plates." *Composite Structures* 95 (2013): 667-675.

Grover N., Maiti D.K. and Singh B.N. "An efficient C0 finite element modeling of an inverse hyperbolic shear deformation theory for the flexural and stability analysis of laminated composite and sandwich plates." *Finite Elements in Analysis and Design* 80 (2014): 11-22.

Grover N., Singh B.N. and Maiti D.K. "A general assessment of a new inverse trigonometric shear deformation theory for laminated composite and sandwich plates using finite element

method." *Proceedings of the Institution of Mechanical Engineers, Part G: Journal of Aerospace Engineering* 228.10 (2014): 1788-1801.

Joshan Y.S., Grover N. and Singh B.N. "Analytical modelling for thermo-mechanical analysis of cross-ply and angle-ply laminated composite plates." *Aerospace Science and Technology* 70 (2017): 137-151.

Joshan Y.S., Grover N. and Singh B.N. "A new non-polynomial four variable shear deformation theory in axiomatic formulation for hygro-thermo-mechanical analysis of laminated composite plates." *Composite Structures* 182 (2017): 685-693.

Mindlin R.H. "Influence of Rotary Inertia and Shear on Flexural Motion of Isotropic Elastic Plates'." *Journal of Applied Mechanics* 18 (1951): 31-38.

Kant T., Ravichandran R.V., Pandya B.N. and Mallikarjuna B.N. "Finite element transient dynamic analysis of isotropic and fibre reinforced composite plates using a higher-order theory." *Composite Structures* 9.4 (1988): 319-342.

Khanna K., Gupta V.K. and Nigam S.P. "Creep analysis of a variable thickness rotating FGM disc using Tresca criterion." *Defence Science Journal* 65.2 (2015): 163.

Khanna, K., Gupta V.K. and Nigam S.P. "Modelling and Analysis of Creep in a Variable Thickness Rotating FGM Disc Using Tresca and von Mises Criteria." *Iranian Journal of Science and Technology, Transactions of Mechanical Engineering* 41.2 (2017): 109-119.

Kulkarni K., Singh B.N. and Maiti D.K. "Analytical solution for bending and buckling analysis of functionally graded plates using inverse trigonometric shear deformation theory." *Composite Structures* 134 (2015): 147-157.

Liu B., Ferreira A.J.M., Xing Y.F. and Neves A.M.A. "Analysis of functionally graded sandwich and laminated shells using a layer-wise theory and a differential quadrature finite element method." *Composite Structures* 136 (2016): 546-553.

Love A.E.H. “The mathematical theory of elasticity.” (1927).

Mantari J.L., Oktem A.S. and Soares C.G. "A new trigonometric shear deformation theory for isotropic, laminated composite and sandwich plates." *International Journal of Solids and Structures* 49.1 (2012): 43-53.

Mantari, J.L. and Soares C.G. "Analysis of isotropic and multilayered plates and shells by using a generalized higher-order shear deformation theory." *Composite Structures* 94.8 (2012): 2640-2656.

Meksi R., Benyoucef S., Mahmoudi A., Tounsi A., Adda Bedia E.A. and Mahmoud S.R. "An analytical solution for bending, buckling and vibration responses of FGM sandwich plates." *Journal of Sandwich Structures & Materials* (2017): 1099636217698443.

Murthy M.V.V. "An improved transverse shear deformation theory for laminated antisotropic plates." (1981).

Na K.S. and Kim J.H. "Three-dimensional thermal buckling analysis of functionally graded materials." *Composites Part B: Engineering* 35.5 (2004): 429-437.

Najafizadeh M.M. and Heydari H.R. "An exact solution for buckling of functionally graded circular plates based on higher order shear deformation plate theory under uniform radial compression." *International Journal of Mechanical Sciences* 50.3 (2008): 603-612.

Nguyen T.K. "A higher-order hyperbolic shear deformation plate model for analysis of functionally graded materials." *International Journal of Mechanics and Materials in Design* 11.2 (2015): 203-219.

Oktem A.S., Mantari J.L. and Soares C.G. "Static response of functionally graded plates and doubly-curved shells based on a higher order shear deformation theory." *European Journal of Mechanics-A/Solids* 36 (2012): 163-172.

Reddy J.N. "A simple higher-order theory for laminated composite plates." *Journal of Applied Mechanics* 51.4 (1984): 745-752.

Reissner E. "The effect of transverse shear deformation on the bending of elastic plates." *Journal of Applied Mechanics* (1945): A69-A77.

Reissner E. and Stavsky Y. "Bending and stretching of certain types of heterogeneous aeolotropic elastic plates." *Journal of applied mechanics* 28.3 (1961): 402-408.

Sofiyev A.H. and Kuruoglu N. "Buckling and vibration of shear deformable functionally graded orthotropic cylindrical shells under external pressures." *Thin-Walled Structures* 78 (2014): 121-130.

Sola A., Bellucci D. and Cannillo V. "Functionally graded materials for orthopedic applications-an update on design and manufacturing." *Biotechnology advances* 34.5 (2016): 504-531.

Thai H.T. and Choi D.H. "An efficient and simple refined theory for buckling analysis of functionally graded plates." *Applied Mathematical Modelling* 36.3 (2012): 1008-1022.

Thai H.T., Nguyen T.K., Vo T.P. and Lee J. "Analysis of functionally graded sandwich plates using a new first-order shear deformation theory." *European Journal of Mechanics-A/Solids* 45 (2014): 211-225.

Woo J. and Meguid S.A. "Nonlinear analysis of functionally graded plates and shallow shells." *International Journal of Solids and Structures* 38.42-43 (2001): 7409-7421.

Web References

[1] http://www.gwultrasonics.com/knowledge/plateshell/

[2] https://www.cnccookbook.com/all-about-milling-composites-part1/

[3] http://www.mdpi.com/1996-1944/5/1/47

Appendix

Stiffness matrix $\left[\overline{R}\right]$

$$R_{11}=A_{11}\alpha^2+A_{66}\beta^2;\ R_{12}=\left(A_{12}+A_{66}\right)\alpha\beta;$$

$$R_{13}=-\left(\frac{A_{11}}{R_1}+\frac{A_{12}}{R_2}+B_{11}\alpha^2+B_{12}\beta^2+2B_{66}\beta\right)\alpha;$$

$$R_{14}=\left(\Omega B_{11}+E_{11}\right)\alpha^2+\left(\Omega B_{66}+E_{66}\right)\beta^2;$$

$$R_{15}=\left(\Omega B_{12}+E_{12}+\Omega B_{66}+E_{66}\right)\alpha\beta;$$

$$R_{22}=A_{22}\beta^2+A_{66}\alpha^2;$$

$$R_{23}=-\left(\frac{A_{21}}{R_1}+\frac{A_{22}}{R_2}+B_{21}\alpha^2+B_{22}\beta^2+2B_{66}\alpha^2\right)\beta;$$

$$R_{24}=\left(\Omega B_{21}+E_{21}+\Omega B_{66}+E_{66}\right)\alpha\beta;$$

$$R_{25}=\left(\Omega B_{22}+E_{22}\right)\beta^2+\left(\Omega B_{66}+E_{66}\right)\alpha^2;$$

$$R_{33}=\frac{A_{11}}{R_1^2}+\frac{A_{12}+A_{21}}{R_1R_2}+\frac{A_{22}}{R_2^2}+\left(\frac{2B_{11}\alpha^2+2B_{12}\beta^2}{R_1}\right)+\left(\frac{2B_{21}\alpha^2+2B_{22}\beta^2}{R_2}\right)$$
$$+\left(D_{11}+D_{12}+D_{21}+4D_{66}\right)\alpha^2+D_{22}\beta^4;$$

$$R_{34}=-\left[\begin{array}{l}\dfrac{\left(\Omega B_{11}+E_{11}\right)\alpha}{R_1}+\dfrac{\left(\Omega B_{21}+E_{21}\right)\alpha}{R_2}+\left(\Omega D_{11}+F_{11}\right)\alpha^3\\+\left(\Omega D_{21}+F_{21}+2\Omega D_{66}+2F_{66}\right)\alpha\beta^2\end{array}\right];$$

$$R_{35}=-\left[\left(\frac{\Omega B_{12}+E_{12}}{R_1}+\frac{\Omega B_{22}+E_{22}}{R_2}\right)\beta+\left(\begin{array}{l}\Omega D_{12}+F_{12}+\\2\left(\Omega D_{66}+F_{66}\right)\end{array}\right)\alpha^2\beta+\left(\Omega D_{22}+F_{22}\right)\beta^3\right];$$

$$R_{44}=\left[\Omega\left(\Omega D_{11}+F_{11}\right)+\Omega F_{11}+H_{11}+\Omega\left(\Omega D_{66}+F_{66}\right)\right]\alpha^2$$
$$+\left(\Omega F_{66}+H_{66}\right)\beta^2+\Omega^2A_{55}+2\Omega K_{55}+L_{55};$$

$$R_{45}=\left[\Omega^2\left(D_{12}+D_{66}\right)+\Omega\left(2F_{12}+H_{12}+2F_{66}+H_{66}\right)\right]\alpha\beta;$$

$$R_{55}=\left[\Omega\left(\Omega D_{22}+F_{22}\right)+\Omega F_{22}+H_{22}\right]\beta^2+\left[\left(\Omega F_{66}+H_{66}\right)+\Omega\left(\Omega D_{66}+F_{66}\right)\right]\alpha^2$$
$$+\Omega^2A_{44}+2\Omega K_{44}+L_{44}$$

$$\left[H\right]=\begin{bmatrix}1&0&0&\xi_3&0&0&g\left(\xi_3\right)&0&0&0&0&0&0\\0&1&0&0&\xi_3&0&0&g\left(\xi_3\right)&0&0&0&0&0\\0&0&1&0&0&\xi_3&0&0&g\left(\xi_3\right)&0&0&0&0\\0&0&0&0&0&0&0&0&0&1&0&g'\left(\xi_3\right)&0\\0&0&0&0&0&0&0&0&0&0&1&0&g'\left(\xi_3\right)\end{bmatrix}$$

$$\varepsilon_1^0 = \frac{\partial u_0}{\partial \xi_1} + \frac{w_0}{R_1};\ \varepsilon_2^0 = \frac{\partial v_0}{\partial \xi_2} + \frac{w_0}{R_2};\ \varepsilon_6^0 = \frac{\partial u_0}{\partial \xi_2} + \frac{\partial v_0}{\partial \xi_1};\ \varepsilon_1^1 = \Omega \frac{\partial \theta_x}{\partial \xi_1} - \frac{\partial \phi_x}{\partial \xi_1};\ \varepsilon_2^1 = \Omega \frac{\partial \theta_y}{\partial \xi_2} - \frac{\partial \phi_y}{\partial \xi_2};$$

$$\varepsilon_6^1 = \Omega\left(\frac{\partial \theta_y}{\partial \xi_1} + \frac{\partial \theta_x}{\partial \xi_2}\right) - \left(\frac{\partial \phi_y}{\partial \xi_1} + \frac{\partial \phi_x}{\partial \xi_2}\right);\ \varepsilon_1^2 = \frac{\partial \theta_x}{\partial \xi_1};\ \varepsilon_2^2 = \frac{\partial \theta_y}{\partial \xi_2};\ \varepsilon_6^2 = \frac{\partial \theta_y}{\partial \xi_1} + \frac{\partial \theta_x}{\partial \xi_2};$$

$$\varepsilon_4^0 = \theta_y;\ \varepsilon_4^3 = \theta_y;\ \varepsilon_5^0 = \theta_x;\ \varepsilon_5^3 = \theta_x$$

Turnitin Originality Report

Processed on: 17-Jul-2018 01:10 +0530
ID: 709704631
Word Count: 8442
Submitted: 14

Ritu Raj Rajpoot By Neeraj Grover

Similarity Index	Similarity by Source
17%	Internet Sources: 6% Publications: 16% Student Papers: 3%

2% match (publications)
Kamlesh Kulkarni, B.N. Singh, D.K. Maiti, "Analytical solution for bending and buckling analysis of functionally graded plates using inverse trigonometric shear deformation theory", Composite Structures, 2015

1% match (Internet from 06-Jan-2015)
http://shellbuckling.com/papers/shellbucklingrefs.docx

1% match (publications)
Neeraj Grover, D.K. Maiti, B.N. Singh, "An efficient C0 finite element modeling of an inverse hyperbolic shear deformation theory for the flexural and stability analysis of laminated composite and sandwich plates", Finite Elements in Analysis and Design, 2014

1% match (publications)
Liu, Bo, A.J.M. Ferreira, Y.F. Xing, and A.M.A. Neves, "Analysis of functionally graded sandwich and laminated shells using a layerwise theory and a differential quadrature finite element method", Composite Structures, 2016.

< 1% match (publications)
Rafik Meksi, Samir Benyoucef, Abdelkader Mahmoudi, Abdelouahed Tounsi, El Abbas Adda Bedia, SR Mahmoud, "An analytical solution for bending, buckling and vibration responses of FGM sandwich plates", Journal of Sandwich Structures & Materials, 2017

< 1% match (publications)
M. Reza Eslami, "Buckling and Postbuckling of Beams, Plates, and Shells", Springer Nature, 2018

< 1% match (Internet from 23-May-2016)
http://nrl.northumbria.ac.uk/14946/1/Thai_et_al__EJMSOL-D-13-00242R1.pdf

< 1% match (publications)
Shyang-Ho Chi, Yen-Ling Chung, "Mechanical behavior of functionally graded material plates under transverse load—Part I: Analysis", International Journal of Solids and Structures, 2006

< 1% match (Internet from 11-May-2016)
http://www.science.gov/topicpages/p/plate+shear+walls.html

< 1% match (publications)
Neeraj Grover, Bhrigu N Singh, Dipak K Maiti, "Free vibration and buckling characteristics of laminated composite and sandwich plates implementing a secant function based shear deformation theory", Proceedings of the Institution of Mechanical Engineers, Part C: Journal of Mechanical Engineering Science, 2014

< 1% match (publications)
A.V. Asha, Shishir Kumar Sahu, "Parametric instability of twisted cross-ply laminated panels", Aerospace Science and Technology, 2011

< 1% match (publications)
Neeraj Grover, D.K. Maiti, B.N. Singh, "A new inverse hyperbolic shear deformation theory for static and buckling analysis of laminated composite and sandwich plates", Composite Structures, 2013

< 1% match (publications)
Ana Neves, "Analysis of laminated and functionally graded plates and shells by a unified formulation and collocation with radial basis functions", Repositório Aberto da Universidade do Porto, 2014.

< 1% match (publications)
Y.S. Joshan, Neeraj Grover, B.N. Singh, "Analytical modelling for thermo-mechanical analysis of cross-ply and angle-ply laminated composite plates", Aerospace Science and Technology, 2017

< 1% match (publications)
J.L. Mantari, "General recommendations to develop 4-unknowns quasi-3D HSDTs to study FGMs", Aerospace Science and Technology, 2016

< 1% match (publications)